VOLUME 15 ISSUE 2

# LIDAR MAGAZINE

SPRING 2025

SPECIAL ISSUE

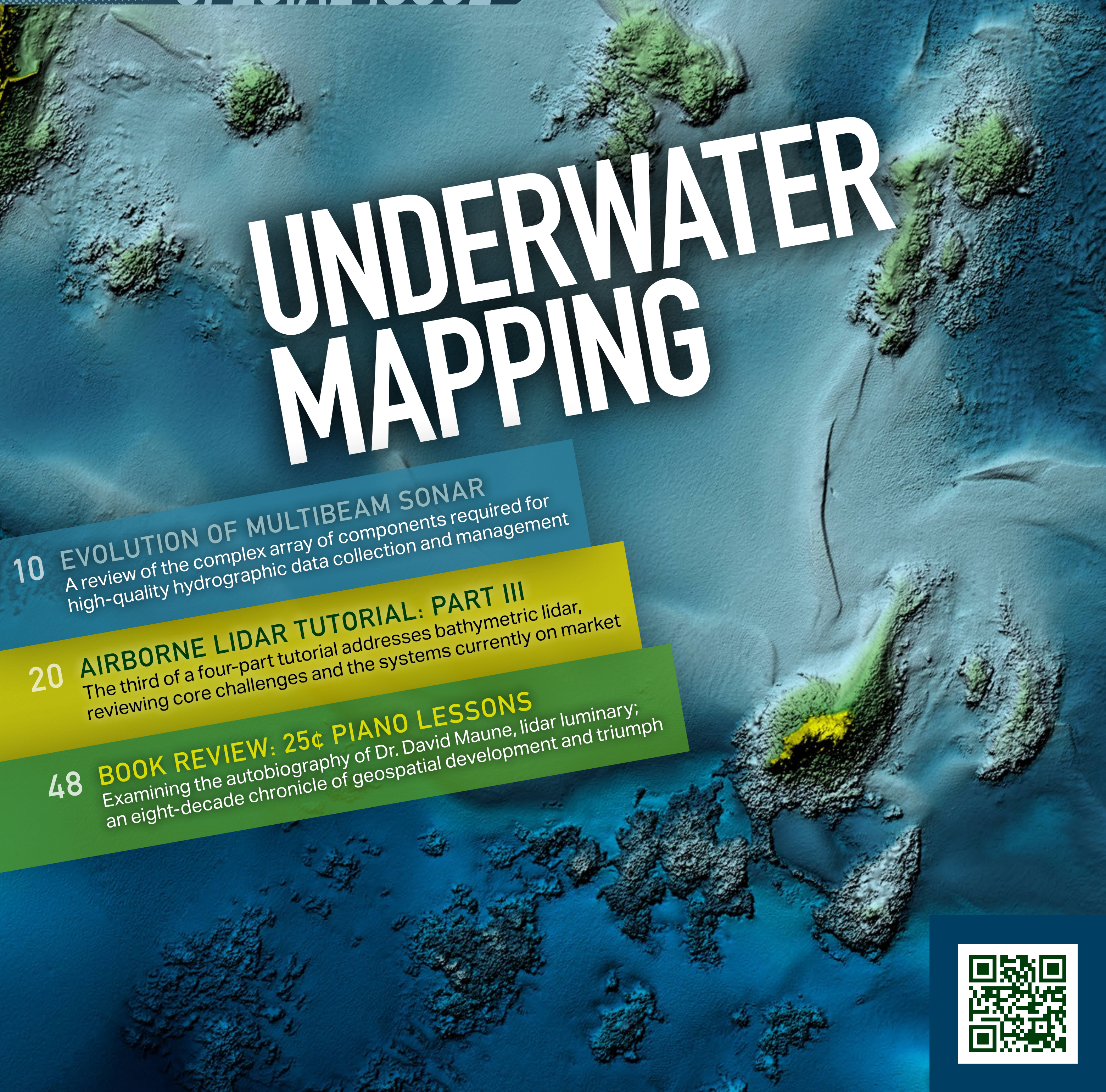

## UNDERWATER MAPPING

# LIDAR MAGAZINE

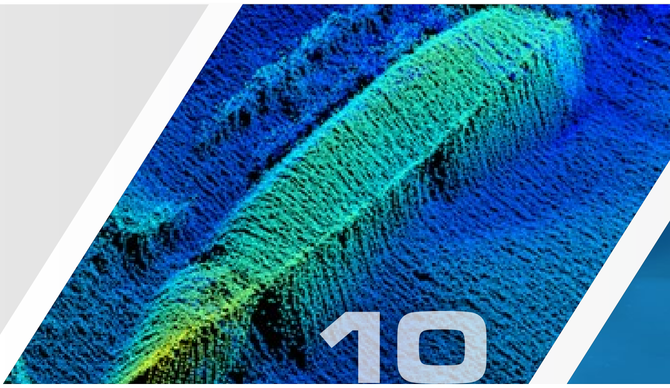


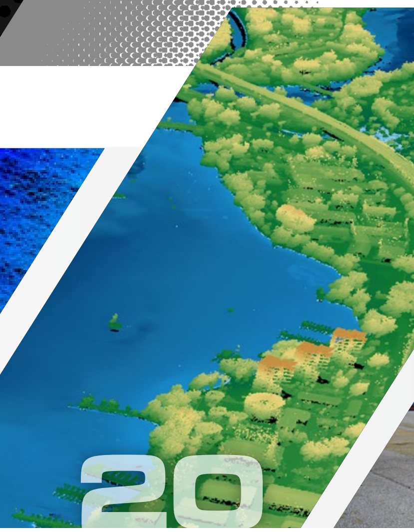



## IN THIS ISSUE



## COLUMNS



**LIDAR To Go!**

Get the most from this magazine on your tablet or laptop.


**◀ ON THE COVER**

*A beautiful example of bathymetric data captured with a Leica Geosystems airborne system.*

DR. A. STEWART WALKER

# All Along the Pipeline

Earlier this spring, I had the good fortune of attending the 59th Photogrammetric Week in Stuttgart[1]. Spectacular in every sense of the word, the biennial meetup colloquially known as PhoWo offered marvelous overviews of the state-of-the-art in photogrammetry, lidar and remote sensing.

After PhoWo, I continued eastwards, to attend the ISPRS Geospatial Week in Dubai, the biggest of the seven United Arab Emirates, an amazing city that has successfully moved its economy away from dependence on oil. I had the privilege of giving travel awards, financed by The ISPRS Foundation, to 22 successful applicants. At this late stage in my career, however, it's gratifying to sit in technical sessions and hear the presentations, many of which are meticulously prepared accounts of high-level work by PhD students and postdocs. In *LIDAR Magazine* we report on new products in the marketplace and on successful projects that companies have completed, but it's fascinating to listen to these enthusiastic young researchers describing investigations that will give rise to the developments that we will see on exhibition booths in the years to come. The next ISPRS Geospatial Week will be hosted by the Polish Society for Photogrammetry and Remote Sensing and the Association of Polish Surveyors in September 2027 in Warsaw, Poland.

On to the articles in this edition. In our last issue, we enjoyed the first "Content to Serve" piece from new contributing writer John Welter[2], where he drew on his knowledge not only on the latest offerings from Hexagon Geosystems but also his frequent interactions with customers around the globe to tease out important trends in the industry. On page 6, we introduce John the person. He has a background of decades of practical experience in the industry, much of it in the family business, North West Geomatics, which was acquired by Hexagon in 2014. We need people who truly understand our complex, fast-moving industry and can explain to us what is happening. John is one of them.

While our principal subject matter is lidar, we like to publish material from time to time on other active sensors, such as synthetic aperture radar, ground penetrating radar, and sonar. Beginning on page 10, Peter Stewart of Trimble Applanix provides an insight on the importance of position and attitude in sonar data acquisition and processing. He also highlights how the user experience with this technology is improving as it evolves.

1 https://lidarmag.com/2025/05/27/59th-photogrammetric-week-stuttgart-1-4-april-2025/

2 Welter, J., 2025. Three key trends influencing the geospatial sector in 2025, *LIDAR Magazine*, 15(1): 46-48, Winter 2025.


LIDAR MAGAZINE

*www.lidarmag.com*

2025 Vol. 15 No. 2



**PUBLISHER** Allen E. Cheves
*publisher@spatialmedia.us*

**MANAGING EDITOR** Dr. A. Stewart Walker
*stewart.walker@lidarmag.com*

**ASSOCIATE PUBLISHER** Kevin Grapes
*kevin.grapes@spatialmedia.us*

**EDITOR EMERITUS** Marc S. Cheves, LS
*marc.cheves@spatialmedia.us*

**CONTRIBUTING WRITERS**
Dr. Qassim Abdullah
Jeff Fagerman
Dr. Juan Fernandez-Diaz
Jason C. Fries
Dr. Al Karlin
Antero Kukko
Aaron Lawrence
Dr. David Maune
Amar Nayegandhi
John Russo
Mike Shillenn
Evon Silvia
Dr. Jason Stoker
John Welter
James Wilder Young
Dr. Michael Zanettii

The staff and contributing writers may be reached via the online message center at our website.

**GRAPHIC DESIGN** LTD Creative, LLC
**WEBMASTER** Joel Cheves
**AUDIENCE DEVELOPMENT** Edward Duff

*LIDAR Magazine* is published 4x annually by Spatial Media LLC. Editorial mailing address: 7820 B Wormans Mill Road, #236 Frederick, MD 21701. Tel: (301) 668-8887; Fax: (301) 695-1538.



*Made in the United States of America*

OFFICIAL PUBLICATION

SPATIAL MEDIA

USIBD U.S. Institute of Building Documentation

# FROM THE EDITOR

Trimble Business Center (TBC) is the subject of an article by three company managers, Khrystyna Bezborodova, Ben Messer and Thomas Widmer. Thomas, a senior product manager, was in the strong team that Trimble fielded in Stuttgart in April. There's a lot more to this article than espousal of Trimble's software leviathan. It explores the customer requirements that drive the innovations and underlines the importance of several developments. It echoes John Welter's assessment of trends, for example how pervasive and essential is AI, especially deep learning, to the rapid extraction of information from data.

On page 20, we bring the third part of Gottfried Mandlburger's tutorial series, "Airborne lidar: a tutorial for 2025." Part III focuses on bathymetric lidar. Gottfried provides a concise, well written introduction to the challenges of lidar measurement through water and examines some of the ways these have been addressed, before exploring some of the systems currently on the market. We are delighted that Gottfried chose to publish this superb didactic material with us and were overjoyed when he cited the series during his invited presentation in Stuttgart.

Our fifth article, found on page 30, shares the thoughts of Walter Lappert, former director of reality capture for Allen3D[3], as he reflects on the role of lidar in discovery, restoration and preservation. Interestingly enough, one of our recent podcast guests was James Rush, Lidar Subject Matter Expert at Allen & Company, Winter Garden, Florida[3]. Allen & Company has a subsidiary, Allen3D, which concentrates on reality capture of the built environment[4].

Another of our contributing writers, Qassim Abdullah, who strides the stage of US lidar and has been instrumental in moving our industry forward in so many ways, is the author of our last article, which begins on page 32, addressing Edition 2, Version 2 (2024) of the *ASPRS Positional Accuracy Standards for Digital Geospatial Data*. Qassim explains the value of RMSE as the gauge of accuracy and describes critical quantities such as horizontal, vertical and 3D accuracy as well as vegetated and non-vegetated measures. The *Standards* have been published in a document that runs to 225 pages, so this article is a useful guide. Indeed, Qassim ends with a summary of the six addenda, which are brimming with information of immense value to practitioners. Like many of Qassim's major contributions, this one is also published in *Photogrammetric Engineering & Remote Sensing* (*PE&RS*). Qassim has been a productive and selfless contributor to both *LIDAR Magazine* and our sister journal, *The American Surveyor*. Indeed, his next piece on the Standards is already in our pipeline.

On page 48, we close with a book review of *25¢ Piano Lessons*, the autobiography of lidar luminary David Maune. *LIDAR Magazine* knows David well and it was a huge privilege to present him in 2018 with the inaugural Lidar Leader Award for Outstanding Personal Achievement. The book is primarily an honest, easy-to-read account of a long, remarkable life. It's not a technical book, but David's geospatial work is a thread throughout, and he provides an appendix with cameos of some of the technologies with which he has worked in a career lasting more than 60 years. There's another appendix on the business uses and benefits of DEMs – for those of us who have known Dave mainly in the 21st century, this encompasses the skills for which he is famous, quantifying these benefits and writing the results into compelling reports on which US government and agencies have acted. The essence of the book, however, is Dave's life story, which revolves round family and friends. In particular, it showcases his resilience as life's slings and arrows have taken their toll over the decades. A wonderful read!

We end with tremendous news. My old friend and colleague, Ron Roth, is joining *LIDAR Magazine* as an associate editor, dissecting news from within the lidar world, as well as relevant geospatial news encountered in the popular press. It's enormously gratifying to read in the mass media accounts where lidar is centerstage, such as a recent piece on flooding and landslides in Kentucky[5]. Ron was a co-founder of lidar start-up Azimuth Corporation in Westford, Massachusetts. We met when we were both involved in the acquisition of Azimuth by LH Systems, part of what is now Hexagon. The Azimuth system became the Leica ALS40 and the rest is history. I well remember customers patiently queueing to talk to Ron on trade show booths all round the world. We welcome him to our group and look forward to his keen analysis of what's going on.

A. Stewart Walker // Managing Editor

3 https://lidarmag.com/podcast_episode/20-james-rush/

4 https://allen3d.digital/

5 https://www.theguardian.com/us-news/2025/may/29/appalachia-kentucky-floods-research-trump-cuts

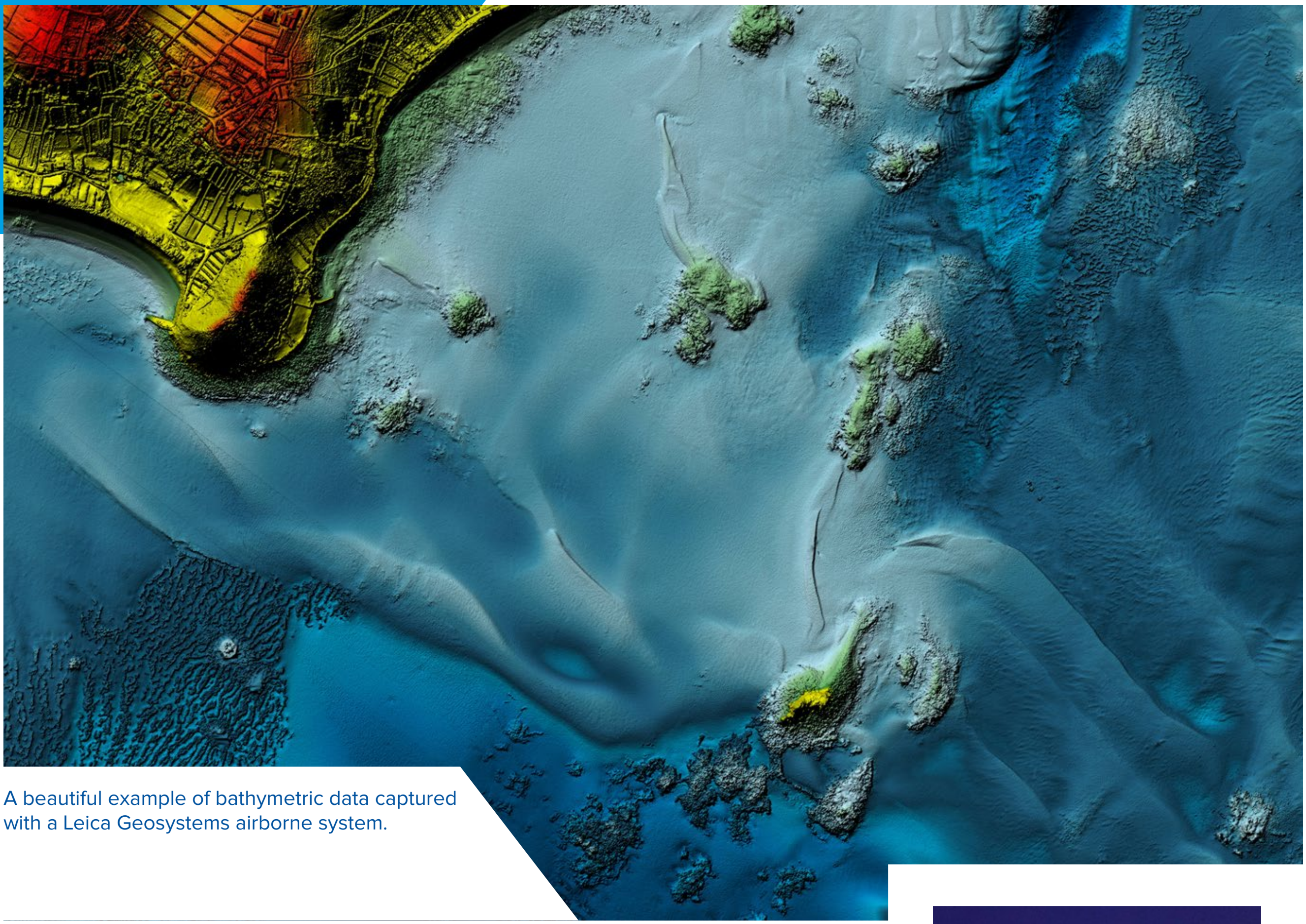

A beautiful example of bathymetric data captured with a Leica Geosystems airborne system.

# New Author Introduction: **John Welter**

*LIDAR Magazine* is pleased to announce that John Welter has joined our team of contributing writers. Based in Arizona, John is President of Geospatial Content Solutions (GCS) at Hexagon's Geosystems division, where he leads the development and distribution of Leica Geosystems' industry-leading airborne sensors. He also oversees the Hexagon Content Program, which has grown into the largest library of aerial imagery and elevation models across North America and Europe.

John brings over three decades of deep industry experience. His expertise spans geospatial services, airborne mapping technologies, IT strategy, and big data – all areas where his leadership and input have left their mark.

With his broad knowledge and passion for progress, John's voice is a welcome addition to the *LIDAR Magazine* community.

BY JOHN **WELTER**

## A family of surveyors

John's introduction to the geospatial world didn't happen in a university lecture hall or graduate program. His father, Fred Welter, was a land surveyor and part of a legacy that stretched across the Yukon, Alberta, and into Alaska, originally through the firm Hosford, Impey & Welter, which eventually spun off into North West Geomatics. As a young boy growing up in this family-run surveying business, John spent summers carrying tripods and maintaining field equipment at North West Geomatics. In his teenage years, John would travel the world as part of a North West Geomatics field crew, working with a Leica RC20/30 aerial film camera on various mapping projects – a summer job that would go on to shape much of his career.

After earning a degree in electronics and systems engineering from North Alberta Insitute of Technology, John began his career. He soon found himself drawn into the family business to pursue innovations in the evolving world of geospatial technology as CTO. The introduction of airborne GPS, automated flight management, softcopy mapping systems, and film scanners positioned North West as one of the technology front-runners in the industry.

## The Hexagon era

North West Geomatics' longstanding partnership with Leica Geosystems set the stage for what would be a natural evolution: Hexagon's acquisition of the company. John had already built strong ties with Leica Geosystems' technical team as North West Geomatics had been an early adopter of the Leica ADS40 airborne digital sensor and among the first to deploy its airborne lidar (ALS) technology. John's North

> "AI enables real-time analysis so that people can monitor subtle environmental changes before they become big issues."

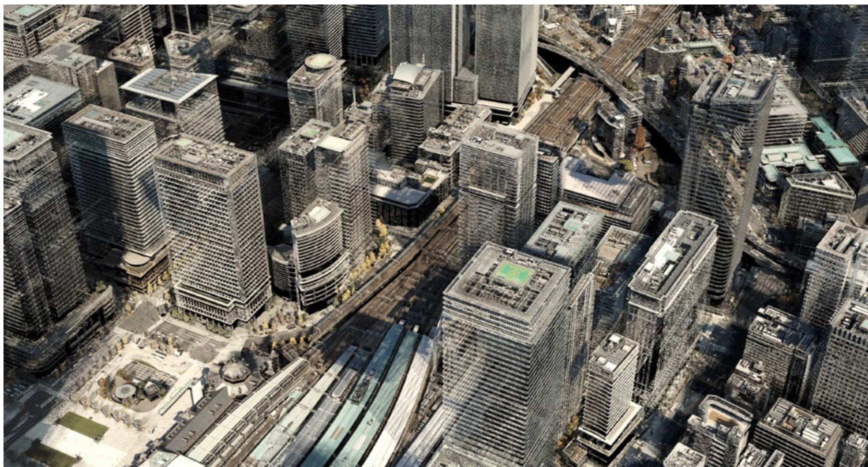

Point cloud captured with Leica CityMapper-2 hybrid system in Tokyo, Japan.

West Geomatics team even developed its own workflow in-house, which would later be commercialized as Leica XPro.

Today, as head of Hexagon's GCS team, John leads a uniquely positioned group that bridges tradition and innovation. On one side is the airborne sensor line, first launched in 1923[1] and now the most established in the industry. On the other is the fast-paced, ten-year-old Content Solutions, designed to deliver large-scale projects quickly and drive innovation through collaborative data-sharing models, such as the Hexagon Content Program[2]. It's a dynamic balance: one half operating in a two-to three-year year product release cycle, the other moving at the pace of two to three weeks – which John says keeps him on his toes.

In his current role, John's mandate is simple yet ambitious: ensure that Hexagon Geosystems' technology – whether sensors, services, or data (and often a combination of all three) – is used on all major mapping programs around the world.

## Leading at the cutting edge

The work John and his team are doing is certainly leading edge. One of the most exciting initiatives in which he has participated is the role of AI in transforming geospatial data from a reactive tool into a proactive one. Previously, remote sensing meant archiving data for use after something bad had happened, like a natural disaster. But now, AI enables real-time analysis so that people can

1 https://lidarmag.com/2023/05/24/100-years-of-innovation-in-heerbrugg/
2 https://hxdr.com/contentprogram/

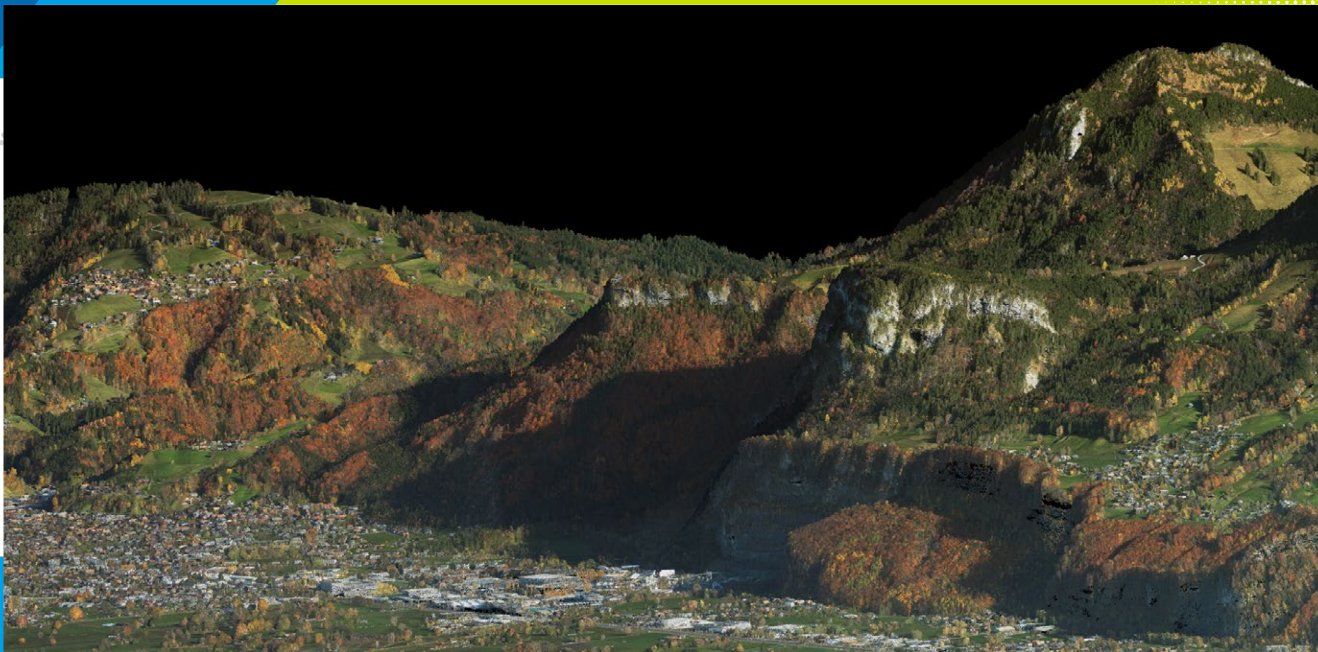

Elevation data captured with Leica TerrainMapper-3 lidar system in Dornbirn, Austria.

monitor subtle environmental changes before they become big issues.

Besides the technology itself, John is motivated by the broader impact it can have on the world we live in. This future-forward thinking is at the heart of R-evolution[3], Hexagon's sustainability-focused arm, where his team and their products play a leading role – for example, mapping Costa Rica's rainforests[4] to preserve biodiversity. These projects reflect a personal mission to help safeguard the planet. He hopes his teenage children will benefit from this and be able to enjoy the results.

## A message to the next generation

For John, the geospatial industry has been a lifelong adventure. While aspiring engineers tend to lean toward big tech, John makes a strong case for pursuing a career in the geospatial industry.

For example, the airborne sensors his team designs are so advanced that some of Hexagon's sub-suppliers use them as R&D testbeds to develop their most advanced solutions.

For those who love technology and want to see the world, John believes there's no better industry. Whether it's collecting data in Colombia, mapping coastlines in Trinidad and Tobago, or overseeing projects in Zimbabwe, his work has offered not only technical challenges but global opportunities. It's a dynamic, high-tech, and rewarding career, one that deserves far more recognition and visibility.

> "While aspiring engineers tend to lean toward big tech, John makes a strong case for pursuing a career in the geospatial industry."

## Lessons that last

John has learned a powerful lesson from his nearly 40 years in the field: never forget the customer. Whether providing sensors, data, or services, success can only come from understanding and supporting the people who rely on the tools you build.

He's less concerned with awards or recognition than with enabling his customers to succeed. For John, the best reward is seeing a customer take a Hexagon solution and apply it in a completely novel way. One example is a customer who recently used its airborne sensor to monitor nighttime light pollution and energy consumption, despite it originally being designed for daytime mapping. Seeing this new application, John's team then worked closely with the customer to improve nighttime surveying performance.

It's these examples of collaboration, creativity, and impact that continue to motivate him. We look forward to sharing more insights from John.

3 https://r-evolution.com/
4 https://lidarmag.com/2024/05/04/digital-twins-open-up-new-possibilities-for-rainforest-conservation/

# The Multi-Faceted Evolution of Multibeam Sonar

## Expanding reach through ease of use

While multibeam sonar solutions have become an essential piece of seafloor and underwater mapping, the application of this technology has been somewhat limited. By and large, this technology integrates highly specialized tools requiring considerable expertise to implement.

The primary challenge to greater adoption lies in the complex array of integrated components, which demand a detailed understanding of the solutions and how they work together. An effective multibeam solution for seafloor mapping includes not just the multibeam sonar, but other pieces like positioning and orientation systems, laser and speed-of-sound sensors, and software to process and manage the data. These components must work together seamlessly to provide high-quality, accurate data in the underwater environment.

BY PETER **STEWART**

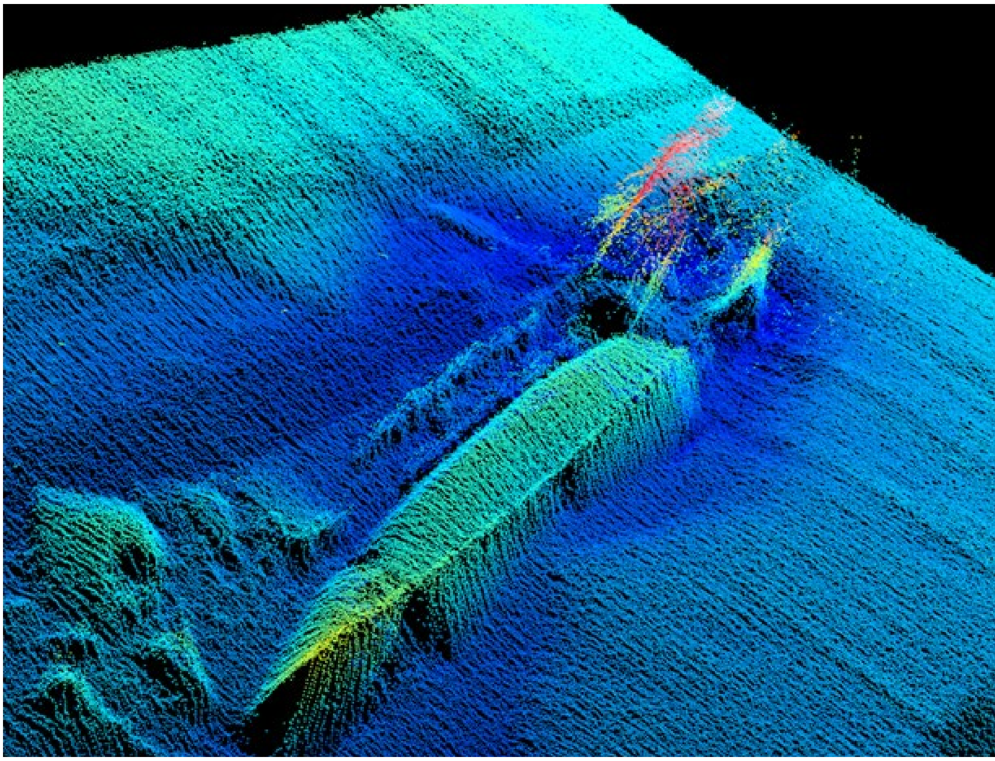

High-quality hydrographic data collection is achieved by integrating position and orientation data from the Applanix POS MV OceanMaster with Trimble RTX, alongside sonar data collected from a multibeam system.

The required level of expertise in understanding these solutions, however, has changed considerably in recent years as technology providers are beginning to deliver more accessible, integrated solutions that prioritize data quality and usability, thus expanding the reach of this technology beyond its traditional hydrographic applications.

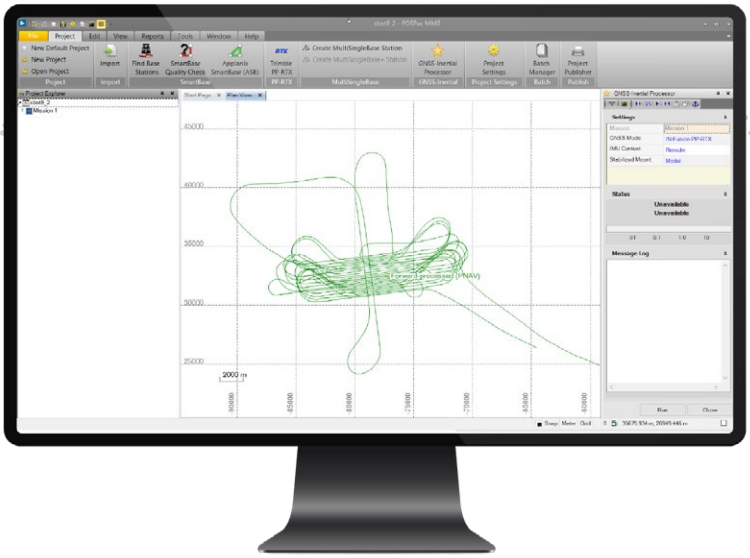

Typical marine vessel data processed in POSPac MMS PP-RTX mode.

There is clear, significant progress towards realizing a multibeam sonar solution so intuitive and user-friendly that using it is as easy as operating a video camera: a tool where operators can immediately access and understand the data, without needing to delve into the technical complexities of configuring the system for the environment. While this idealistic vision of simplicity is closer to reality than ever before, current multibeam capabilities still require some considerable forethought to achieve the desired accuracy.

## A POS perspective

The evolution of position and orientation systems (POS) provides some insights into the evolution of multibeam solutions. For example, Trimble® Applanix's POS MV™ off-the-shelf commercial product is uniquely suited to the requirements of precision marine motion sensing, hydrographic surveying and charting. It delivers precise position, heading, attitude, heave and velocity data for a marine vessel and remote sensing equipment. By combining GNSS data with angular rate and acceleration derived from an inertial measurement unit (IMU), along with GNSS Azimuth Measurement System (GAMS) heading, it offers an accurate six-degrees-of-freedom positioning and orientation solution. When this is combined with multibeam sonar, hydrographers can generate very precise, georeferenced seafloor mapping data.

Manufacturers such as Trimble Applanix have devoted considerable time helping customers integrate and configure system components at the factory and during commissioning. These tasks include understanding critical factors such as:

- Timing - ensuring the timing of data from different sensors is properly synchronized
- Datums - understanding the datums being used and how they need to align
- Offsets - precisely measuring the physical offsets between sensors on the vessel
- Misalignment angles - measuring and accounting for any angular misalignments between sensors

By resolving these factors and setting up the multibeam system prior to deployment, users can experience a more seamless flow of data across a fully integrated solution, thereby providing real-time or near real-time results so that hydrographers as well as marine contractors can quickly understand what's happening under the surface without having a deep understanding of the system itself.

The key innovations on which developers have focused include improving data availability and quality through the deployment of a seamless GNSS solution that integrates sensor calibration and correction technologies with multibeam sonar.

## A port of possibility

The Port of London project provides an example of this combined technology. The Port of London Authority is charged with ensuring navigational safety and port security along the River Thames, a complex survey area with a number of bridges, considerable river traffic and other obstructions that block GNSS line of sight.

Tasked with collecting survey data, the Port of London Hydrographic Service equipped its vessel with a POS MV OceanMaster GNSS-aided inertial navigation system for georeferencing the NORBIT multibeam sonar and a lidar sensor.

The survey team sought to demonstrate the performance improvements to be gained from the Trimble Applanix IN-Fusion+ technology for direct georeferencing of multibeam data. A comparison with previous techniques was undertaken, and the performance improvements were clear, especially in areas immediately around bridges.

With a fully integrated solution, the team was able to capture lidar and multibeam sensor data at the same time in order to map both the structural elements on the underside of a bridge and the underwater view, providing complete, accurate information in areas where the GNSS environment makes it most difficult to do so, but where, conversely,

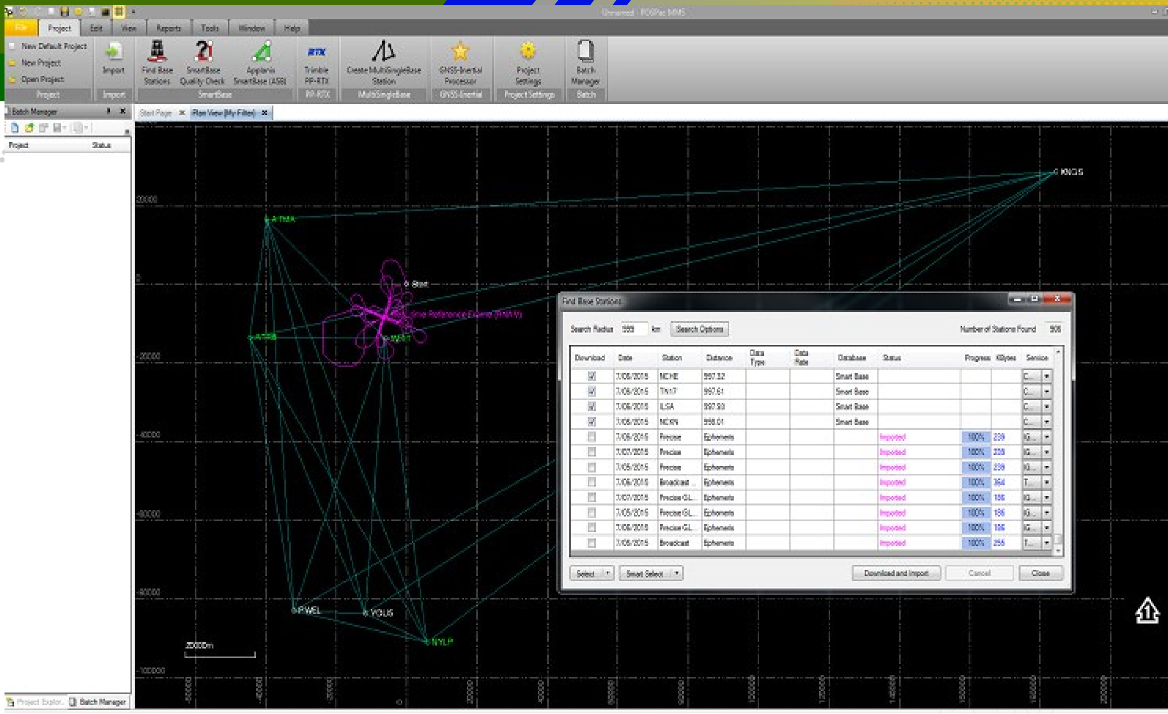


POSPac MMS includes a database of thousands of GNSS base stations worldwide, which can be automatically downloaded for single or SmartBase processing.

the need for accuracy is at its highest. Impressive results were obtained, with demonstrable improvements in mapping uncertainty.

On another project, PPP techniques provided centimeter accuracy independent of access to base stations. In this case, the Port of London Hydrographic Service collected data from the vessel *Maplin*, which is equipped with a POS MV OceanMaster GNSS-aided inertial navigation system for georeferencing the R2Sonic™ 2024 multibeam sonar. HYPACK™ software was used for data acquisition, and Fledermaus™, for the visualization of some results.

The data was collected in the Thames Estuary, where Ordnance Survey OSNet GNSS reference stations provide the data necessary to compute a SmartBase post-processed VRS network.

The Applanix SmartBase (ASB) technology allows the computation of position to centimeter accuracy, with distances to the nearest reference station on the order of 20-60 km. A comparison was then done between the ASB solution and that from PP-RTX. An area in the outer Thames Estuary provided an ideal location to compare the known accuracy of a SmartBase PPK solution with PP-RTX.

The PP-RTX post-processed approach achieved an impressive accuracy of 0.019 m, 0.021 m and 0.049 m RMSE in X, Y and Z respectively – and did so without using local reference stations. The PP-RTX post-processed approach provides a number of advantages including almost no convergence time and no need for local reference stations. The processed data is available within one hour after collection, which facilitates a fast turnaround of the mapping solution, ensuring deadlines can be met while providing reliable accuracy.

## Inertial directions

For marine construction and asset-monitoring applications, surveys such as those undertaken by the Port of London provide a powerful modern approach to multibeam data gathering and ease of use.

Combining a real-time correction service or post-processing techniques with multibeam sonar allows surveyors and contractors to maintain the necessary data quality and accuracy for real-time construction applications such as monitoring dredging operations in challenging environments with limited sky visibility. One key is leveraging multiple technologies to ensure that the data remains usable and of high quality, even in obstructed construction sites and dredging areas, while ensuring the integration is seamless, simple and robust.

In the near future, complete multibeam solutions with more seamless integration of GNSS, inertial and other technologies such as lidar will make the technology more accessible to a wider audience, beyond just expert hydrographic surveyors, so that it can be applied to construction, environmental monitoring, search and rescue, and more. These cleaner, simpler, cloud-based, automated processing techniques makes hands-off and remote operations more attainable…a much needed workflow for the future.

**Peter Stewart** is director of marine products at Trimble Applanix. He is responsible for product development and the implementation of business strategies for the company's marine solutions.

LP360

# Maximize Your DJI L1/L2 Workflow with this LP360 Bundle

Process, analyze, and maximize L1/L2 LiDAR survey data, producing valuable information and deliverables

Manage your coordinate system

Advanced tools

LP360 Cloud Extension

QC/QA your data

## LP360 Drone bundle for DJI Users

Are you using the DJI Zenmuse L1 or L2 LiDAR and RGB solution to capture 3D data for aerial surveying?

LP360 Drone's DJI L1/L2 Cloud Batch Processing Add-On streamlines your DJI data processing workflow by allowing you to process L1/L2 raw LiDAR data directly in LP360 Drone, eliminating the need for DJI Terra. With LP360 Drone you can process, analyze, and maximize your L1 & L2 drone survey data, creating enhanced and highly accurate deliverables.

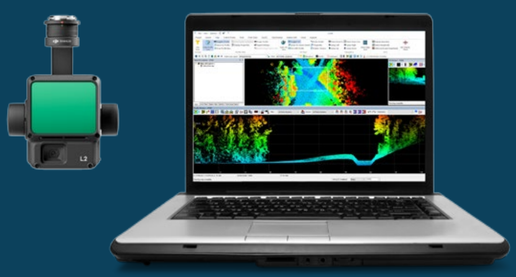

**Get Started Now!**

Scan this QR Code and learn more about the LP360 bundle for DJI Users

**$3,850**

USD/Year

**Includes:**

· LP360 Drone
· Strip Align for Drone
· DJI L1/L2 Cloud Batch Processing

# Connected Workflows Optimize Value of Geospatial Data

New features in Trimble Business Center (TBC) offer advanced capabilities that boost efficiency, improve output, and open new markets by including artificial intelligence to streamline classification and feature extraction processes, as well as photogrammetric tools to produce high-accuracy aerial data products.

BY KHRYSTYNA **BEZBORODOVA,** BEN **MESSER,** AND THOMAS **WIDMER**

Investment in geospatial technology is driven by the desire to make better decisions based on complete and accurate information. Continued advances in reality capture data with mobile mapping systems, drones, 3D laser scanners, and other tools create demand for software capable of fully leveraging the data. New capabilities in Trimble Business Center (TBC) integrate artificial intelligence (AI) and connected workflows to facilitate the efficient extraction of information from multiple types of data and connect multiple users to one data management environment that unlocks the true value for a broad range of users.

## Responding to industry trends

TBC's evolution reflects industry trends, such as a shift to doing business in the cloud and widespread demand for faster and more accurate information. New features improve access to data, increase efficiency and productivity, offer better visibility and transparency, and support decision-making by providing more informed insights.

The key focus on integrating diverse data types addresses the surge in mixed-reality applications and the proliferation of various sensors. Capabilities that support processing a wide array of data inputs ensure the platform remains compatible and flexible for all users, aligning with the changing landscape of surveying technology.

The latest enhancements for the office emphasize connected workflows to encourage data sharing throughout the ecosystem. A single source of truth is created by combining various data sets. Integrating data from multiple sources, such as mobile mapping systems, terrestrial scanners, and drones, results in richer and more intelligent deliverables, including accurate 3D models and digital twins that support design and construction projects.

Cloud-based integration is supported by functionality to transfer massive reality-capture data sets. TBC is the only application capable of uploading panoramic imagery and point cloud data from any source as one data set to the Trimble Connect cloud-based common data environment. Within Trimble Connect, multiple desktop and cloud applications from various manufacturers can be used together.

The recently launched Trimble Reality Capture Platform Service (TRCPS), an extension of Trimble Connect, is a secure web-based solution that facilitates effective collaboration among stakeholders, maintains data integrity, and enables multiple platforms to connect to one service. By democratizing access to scanning data, TRCPS helps the geospatial footprint reach a wider audience in the office. Early usage statistics show that for every one person contributing scan data, there are 10 people consuming the data, which extends the utility of point clouds.

When it comes to aerial photogrammetry features, continued development is directly influenced by a commitment to sensor fusion—leveraging multiple sensors within a single solution—to eliminate the need for multiple products.

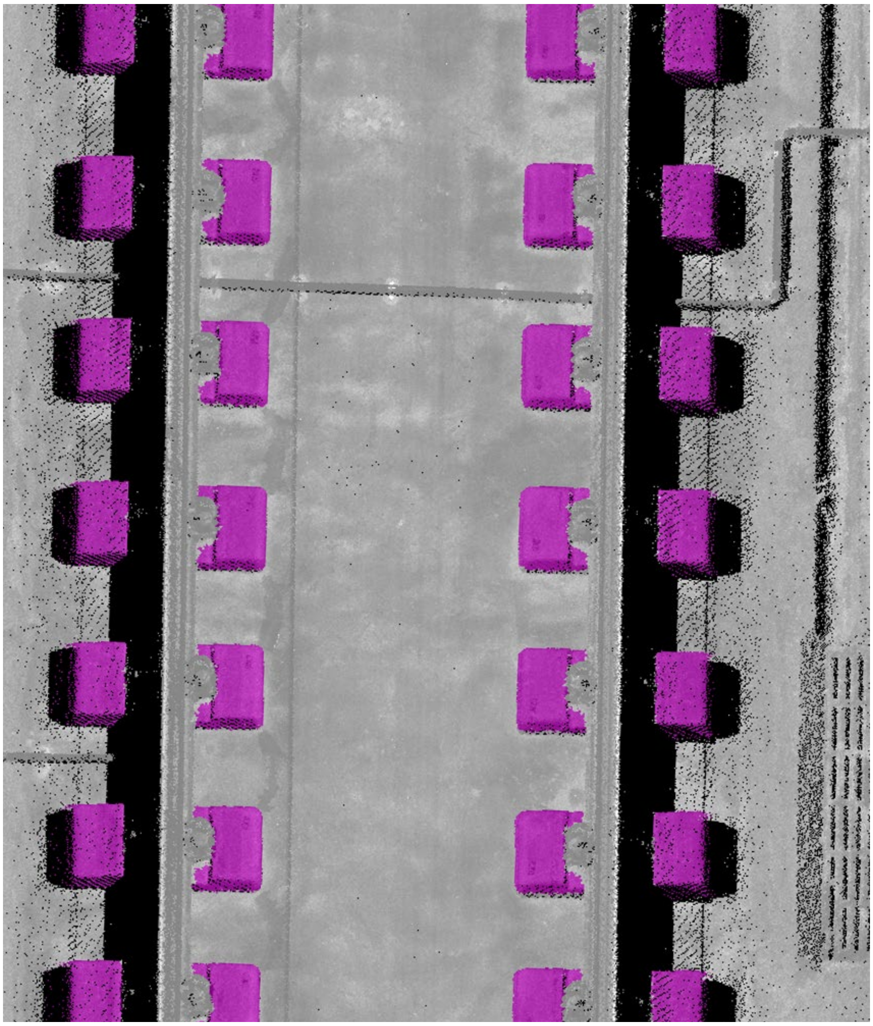

Rhomberg Sersa Rail AG

A new tool in TBC software was used to train 3D deep learning models to extract rail sleepers from the point cloud.

### AI's growing role in generating data insights

Software is evolving to keep up with advances in hardware that produce massive volumes of data. To fully leverage the new data collection technologies, AI-based feature extraction and classification tools are critical. The pioneering use of AI in data processing is propelling TBC towards incorporating smarter algorithms that can automate routine tasks, enhance data accuracy, and streamline processing times. Meeting the rapidly growing demand for geospatial information in many industries relies on software to enable flexible, customizable automation workflows.

The user already has the ability to generate information for many types of analysis, but AI gives more tool options and faster and better results. This includes AI-based capabilities for automated point-cloud classification, automated extraction of asset geometry and attributes, and complex domain-specific analysis workflows such as tockpile management in earthwork projects and pavement condition inspection. Automated processes advance existing workflows and create more powerful tools that require minimum user interaction for monotonous tasks, such as the introduction of an AI model for fully automated extraction of lane lines from mobile mapping data.

Software today offers tools and workflows that satisfy the standard requirements of most surveying and construction projects, but customers with non-standard, unique, domain- or location-specific requirements need additional resources. TBC includes capabilities for custom training of classification AI models and generic CAD point extraction for objects in point clouds from any sensor. By customizing workflows, users can create their own intellectual property (IP) and

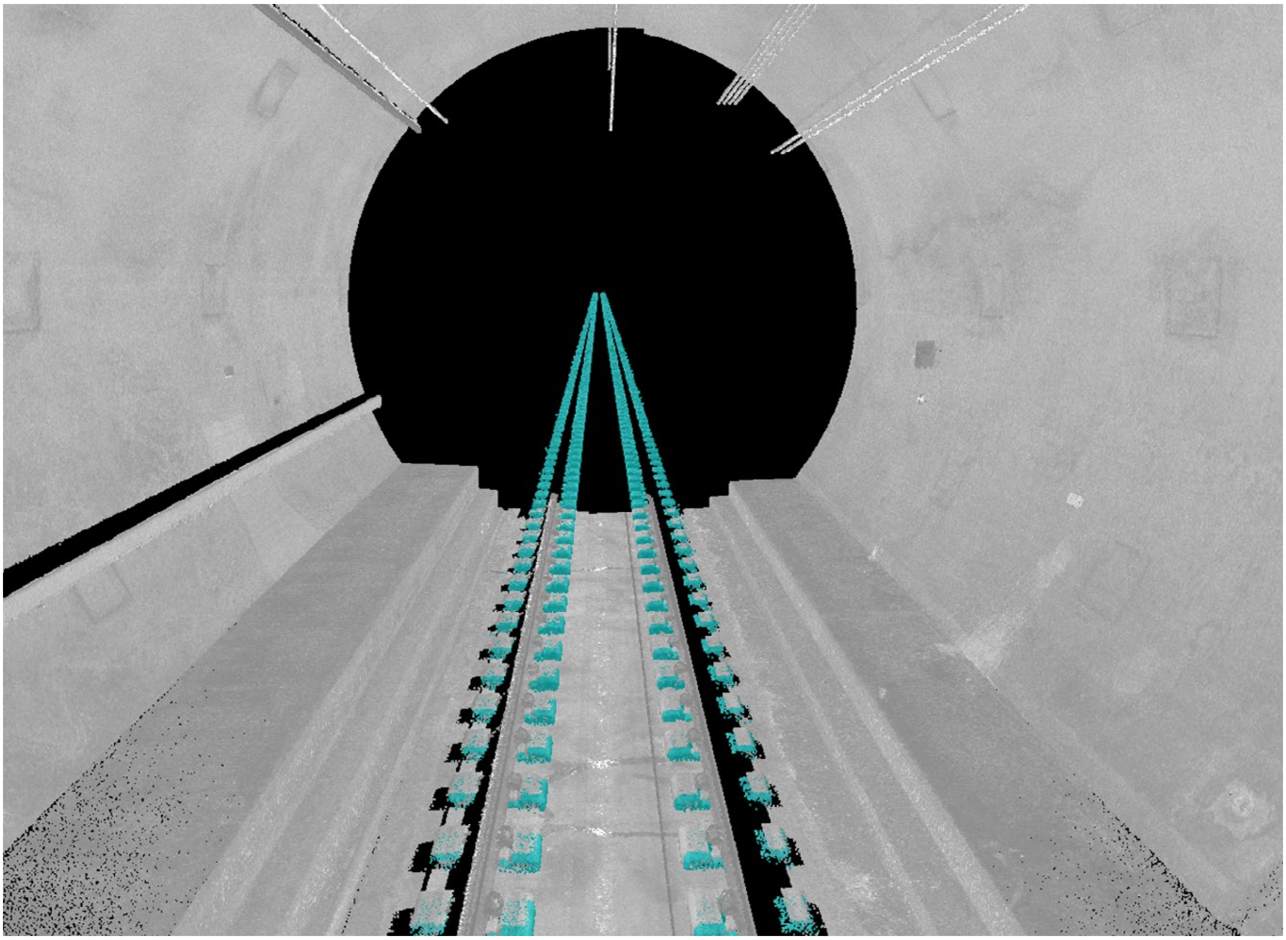
Rhomberg Sersa Rail AG

Spacing between each pair of sleepers was checked to verify that the gap fell within the required tolerance.

offer unique and personalized services to their customers, distinguishing themselves in a market where everyone has standard pre-built tools.

## Capabilities in practice

- GeoVerra, one of Canada's most established land surveying and geomatics firms, uses a powerful combination of mobile mapping, AI processing and trained models in TBC to complete transportation projects with speed and precision while setting new standards for project delivery. "We see at least 30 percent time savings on large projects when performing feature extraction and classification in TBC," says Alex Garcia, GeoVerra's national manager of mobile solutions. "The comprehensive information generated adds value and helps us meet and often exceed customer expectations."

  At Trimble Dimensions 2024, GeoVerra described how they are leading the way in the transportation industry by utilizing mobile mapping systems for fast, safe, and accurate geospatial data collection. They are also training unique AI models in TBC for classification and extraction of assets in airports, railway and roads for better data accuracy and workflow efficiency.
- Rhomberg Sersa Rail Group (RSRG), another innovative technology company, is adopting new methods of monitoring, inspecting and analyzing rail infrastructure during and after construction to improve safety and assist with long-term lifecycle management. At the Gotthard Base Tunnel in Switzerland, AI models in TBC were trained to automatically extract 20,000 rail sleepers (railroad

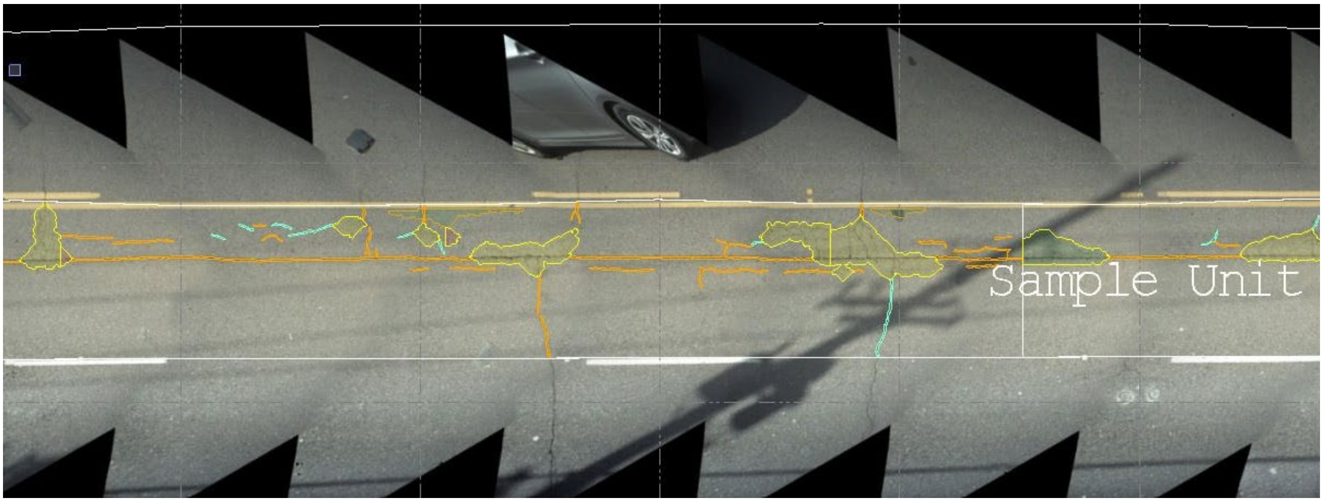


GeoVerra

Pavement inspection functionality in TBC automatically extracts distresses and calculates Pavement Condition Index.

ties) that had been installed in the tunnel, drastically reducing the time needed to identify anomalies.

"TBC offered the capability to train AI for a specific type of sleeper and improve the results, which allowed us to automate the extraction process and complete the work quickly with confidence," said Dimitrios Kyritsis, RSRG's digital rail services manager. "We were pleased with our 97% accuracy after training the model."

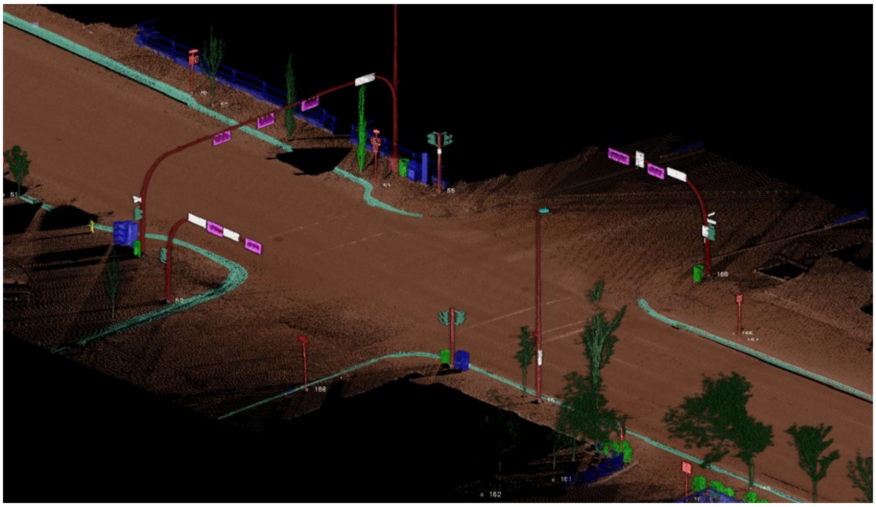

GeoVerra

3D deep-learning models were trained to extract features such as curbs, trash cans, traffic lights and sign plates using TBC.

## Transforming pavement and roadway asset inspection

With the goals of improving work zone safety and transportation user safety, and decreasing asset maintenance costs, new end-to-end workflows are changing the way pavement and roadway data is collected and processed. More frequent and detailed condition information is now available through the use of mobile mapping systems and software that turns this data into information.

Vehicle-mounted mobile mapping systems are ideal for large linear projects. Workers safely drive at normal speeds without costly road closures while high-resolution 360-degree cameras and dual laser scanners capture comprehensive information about pavement and roadway assets.

A key area of functionality for the transportation infrastructure industry is the seamless workflow that connects data collection, data processing/information extraction, and management of this information for budgeting and decision-making. TBC automatically extracts information about the location and severity of each pothole and rutting, corrugation, depression, bump, shoulder drop-off, different types of cracking, etc. In addition to detection, TBC evaluates the severity of each defect and ties the location of defects to segments within each analyzed road section.

The International Roughness Index (IRI) and Pavement Condition Index (PCI) are calculated for pavement inspection reporting. The condition information can then be consumed by Trimble AgileAssets software, which provides advanced analytics to support data-driven decisions across the infrastructure, or any other asset lifecycle management software.

The comprehensive pavement management ecosystem allows for efficient data collection, analysis, and management, and supports proactive instead of reactive asset management for additional cost and time savings. Fixing issues before they become driving hazards protects employees and transportation users while decreasing the cost of asset maintenance.

Transportation asset management is an important application area for TBC's feature extraction and classification tool. By implementing the pavement analysis workflows, users can analyze many miles of pavement significantly faster compared to traditional methods.

Automated AI workflows deliver more granular information with higher accuracy and produce more consistent and objective analysis, producing better results compared to traditional methods. The combination of efficient data collection and AI processing is key to delivering an effective asset management program.

## Demand grows for enhanced aerial photogrammetry support

Photogrammetry has become indispensable in surveying. Today, it's rare to find a surveyor without a drone ready at hand. TBC's mission is to make integration of drone data into existing projects as straightforward as possible. The platform is designed for ease of use, enabling surveyors to incorporate drone data seamlessly into their daily routines.

The demand for 2.5D and 3D photogrammetry models is expanding across various industries, from construction and urban planning to inspection, data preparation, and monitoring. The TBC team is supporting this need with a commitment to accuracy, automation, and simplicity. By continuously refining TBC algorithms to meet the demand for higher precision, customers have access to state-of-the-art photogrammetric technology.

The photogrammetry module in TBC includes extensive functionality originally developed in Trimble Inpho software. These features support importing data from a broad range of drones and aggregating the aerial data with other survey data to produce comprehensive photogrammetric 3D deliverables.

The processing of drone imagery using the photogrammetry module is effective for complex projects, including those with oblique and nadir imagery. The resulting 3D point clouds and meshes enable the processing of structural inspection projects, such as bridges, open-pit mines and dams.

## Bringing more value to data

The shift towards remote work and the need for cloud-based solutions for team collaboration are reshaping surveying workflows. Real-time data sharing, cloud computing, and collaborative project management are just the beginning.

Analysis and report generation are enhanced by the ability to receive data from multiple sources, process that data, and interact with other software within and outside the ecosystem. Whether it's aerial, terrestrial, mobile mapping, or tunneling data, these tools elevate data processing capabilities, while the connected workflow significantly improves communication and transparency between all stakeholders with unprecedented speed and accuracy.

New AI-based functionality for classification and feature extraction minimizes the drudgery to make geospatial professionals more efficient and reliable, while the additions to the photogrammetry module offer advanced processing of aerial imagery for inclusion in 3D models and digital twins. Innovative software truly reveals the value of the data by extracting valuable insights with high accuracy and speed and generating actionable information.

---

**Khrystyna Bezborodova** is a feature extraction product manager at Trimble Geospatial. She coordinates teams across Trimble Business Center, Trimble Photogrammetry, eCognition, Mobile Mapping, Scanning and Central AI to deliver point cloud and image-based geometry and attribute deliverables for survey and construction workflows.

---

**Ben Messer** is a product manager for Trimble Business Center. His responsibilities include overseeing the development and enhancement of TBC while ensuring that the needs of survey and construction professionals are met. He works closely with the development team and other TBC product managers to prioritize features, gather user feedback, and guide the overall product strategy to deliver a comprehensive office software solution.

---

**Thomas Widmer** is senior product manager for Trimble Photogrammetry. He focuses on the integration of photogrammetric solutions for nationwide aerial image projects (Trimble Inpho) and photogrammetry solutions for the surveying market. Thomas has worked for over 20 years as a support, trainer, and consulting engineer for Trimble Inpho.

# AIRBORNE LIDAR

# A Tutorial for 2025

## Part III: Bathymetric lidar

Airborne laser bathymetry (ALB), also referred to as bathymetric laser scanning or bathymetric lidar, is a technique to measure the depths of shallow coastal or inland water using a pulsed, scanning laser. While the infrared wavelengths used for topographic lidar cannot penetrate water, wavelengths in the green and blue spectrum of visible light are suitable, as signal attenuation is least for wavelengths around 460-550 nm. Most bathymetric lidar sensors use a wavelength of λ=532 nm, which is the result of frequency-doubling a conventional Nd:YAG infrared laser operating at λ=1064 nm. Since the invention of lasers in the 1960s, there have also been reports on the use of green lasers. While underwater object detection was the first application, ALB is mostly used today for surveying and monitoring shallow coastal areas, harbor facilities, and shipping channels. The increased measurement rates of today's sensors also allow the use of this active remote sensing method for the mapping and monitoring of smaller standing or running inland waters.

### Measuring principle

A laser mounted on an airborne platform (fixed-wing aircraft, helicopter, unmanned aerial vehicle) emits very short laser pulses in the green wavelength range. The laser pulse passes through the atmosphere, possibly interacts with objects above the body of water (vegetation, power lines, etc.) and then hits the water surface. There, the laser beam is reflected on the one hand and refracted on the other when it enters the optically denser medium of water at the air-water interface. The direction of the deflected beam depends on the incidence angle at the water surface and on the refractive indices in air and water. The relation between incoming (air-sided) and outgoing (water-sided) ray direction and speed of light is described by Snell's law of refraction:

$$\frac{\sin \alpha_L}{\sin \alpha_W} = \frac{n_W}{n_L} = \frac{c_L}{c_W} \quad \text{EQ1}$$

$\alpha_L$ and $\alpha_W$ denote the angles between the water surface normal direction and the air-sided ($\alpha_L$) and water-sided ($\alpha_W$) laser beam, $c_L$ and $c_W$ are the laser pulse propagation velocities in air and water, and $n_L$ and $n_W$ are the corresponding refractive indices. The refractive index in a vacuum is 1.0, in dry air (15 °C, 1013.25 mbar) around 1.0003, and in clear water 1.333. Please note that the refractive index in water is slightly different for angular deflection and the propagation velocity. For the former, the phase velocity of the inherent laser light is crucial, and for the latter, the group velocity of the laser pulse.

Within the water column, the laser light interacts with the water and suspended sediment particles, and the signal is both scattered and absorbed. Continuous forward scattering leads to a hyperbolic conical expansion of the laser spot size with increasing water depth. Volume backscattering, in turn, causes reflection of the laser signal from the water column back to the receiver, where the recorded amplitude drops asymmetrically after the first peak from the water surface. Part of the laser radiation finally reaches the bottom of the water body (seabed, river bottom, etc.), where it is reflected and partially

BY GOTTFRIED MANDLBURGER

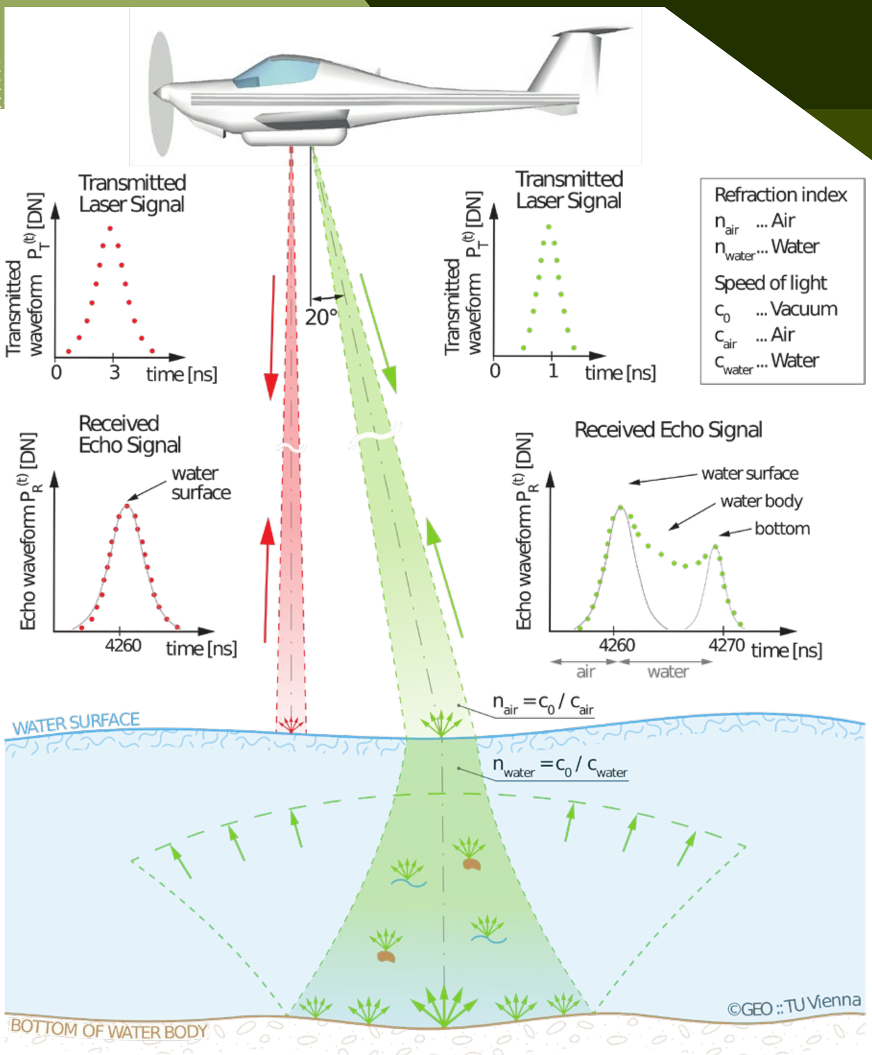


**Figure 1:** Setup and specifications of selected integrated lidar-camera sensors; laser footprint and image GSD are reported for a flying altitude of 1000 m.

absorbed, depending on the reflectance of the bottom material. After the return trip through the water column and atmosphere, a small proportion of the emitted radiation reflected from the bottom reaches the receiver. In a similar way to topographic laser scanning, the roundtrip time can be measured by registering the time stamps of the emitted pulse and the received echo (discrete echo systems). Due to the complex interaction of the radiation at the air-water interface, in the water columns, and at the bottom, however, most of the available ALB sensors record the entire waveform (outgoing pulse and received echo response) discretized in time with a sampling rate of 1-5 GHz. The waveforms can be evaluated either online during the flight or in post-processing, if the digitized signal is also stored on disk. In both cases, waveform analysis provides radiometric information in addition to the roundtrip time (distance). Next to the measurement range, the signal intensity depends on atmospheric parameters (humidity), roughness of the water surface, water turbidity, water depth, and reflectivity of the bottom surface. The relationships are schematically sketched in **Figure 1**.

## Interaction of laser light with water

In Part I of this tutorial, we discussed the general relation between the transmitted power $P_T$ and the received power $P_R$ . For extended targets, i.e. targets larger than the laser footprint, we can simplify the laser-radar equation as:

$$P_R = \frac{P_{Tf}}{4\pi R^2}\,\sigma + P_{BK} \qquad \text{EQ2}$$

In Equation 2, $P_{Tf}$ summarizes all parameters, which can be considered constant for a single flight mission, namely the transmitted power $P_T$, the diameter of receiver's aperture $D$, and the atmospheric and sensor-specific loss factors $\eta_{ATM}$ and $\eta_{SYS}$.

$$P_{Tf} = P_T\, D^2\, \eta_{ATM}\, \eta_{SYS} \qquad \text{EQ3}$$

The remaining parameters influencing the received power $P_R$ are the measurement range $R$ and the backscattering cross-section σ. The latter incorporates all target properties, i.e. reflectance and backscattering solid angle (cf. Part I, Equation 3).

Attenuation of the laser radiation occurs within the atmosphere, but for the most part in the medium of water. As stated above, when the green laser signal hits the water surface, part of the signal is reflected at the air-water interface, while the remaining part penetrates the water body and reflects off the bottom. For laser beams hitting water, we can further separate the signal contributions from the water surface ($P_{WS}$), the water column ($P_{WC}$), the bottom of the water body ($P_{WB}$), and background radiation $P_{BK}$.

$$P_R = P_{WS} + P_{WC} + P_{WB} + P_{BK} \quad \text{EQ4}$$

The following Equations 5-7 describe the individual contributions from (i) the water surface, (ii) the water column, and (iii) the water bottom, summarized in Equation 4:

$$P_{WS} = \frac{P_{Tf} L_O}{4R^2} \quad \text{EQ5}$$

$$P_{WC}(r_w) = \frac{P_{Tf} F (1 - L_O)^2 \beta(\varphi) e^{-2kr_w}}{4(n_W R + r_w)^2} \quad \text{EQ6}$$

$$P_{WB}(r_w) = \frac{P_{Tf} F (1 - L_O)^2 R_B e^{-2kr_w}}{4(n_W R + r_w)^2} \quad \text{EQ7}$$

The fraction of the total received signal strength reflected from the water surface $P_{WS}$ is described by surface albedo $L_O$, which in turn depends on the roughness of the water surface and the incidence angle between the laser beam and the water surface normal direction. As laser beams hitting the water surface orthogonally produce a very strong backscatter, which may lead to saturation at the receiver, bathymetric laser scanners typically employ conical scanning with a constant off-nadir angle of around 15-20°. Due to the high proportion of specular reflection, direct reflections from the water surface can only be detected when the surface is slightly ruffled. $P_{WS}$ is also dependent on the volume scattering function β(ϕ).

The signal from the water column $P_{WC}$ depends on the underwater measurement range $r_w$ and is dominated by scattering and absorption described by the diffuse attenuation coefficient $k$ that characterizes the optical properties of water (i.e. turbidity). $n_w$ is the refractive index of water and is a loss factor to account for the fact that not all of the backscattered energy reaches the detector (see **Figure 1**). In addition to all the parameters described above, the contribution from the water bottom $P_{WB}$ is influenced by the seabed reflectance $R_B$. Light-colored sand (coastal areas) or gravel (inland rivers) have a high reflectivity and thus favor depth penetration. In contrast, muddy soil or dark, submerged vegetation have a negative effect on the achievable depth.

## Refraction correction

As explained above, laser bathymetry is a two-media measurement method. The laser beam is deflected at the air-water interface and the propagation speed decreases on entering the optically denser medium of water. For the calculation of precise 3D point coordinates of the water bottom, the intersection point of the laser beam with the water surface must be determined for each laser pulse. In addition, the magnitude and orientation of the tilt of the water surface are also required. The refraction point can be determined individually for each laser pulse, if both the water surface and the water bottom can be identified from the waveform of the backscattered echo signal. This is especially the case for the classic ALB sensor design with coaxial emission of the primary infrared and the green laser radiation derived from it. The infrared channel provides information from the water surface, but does not penetrate the water body. The green channel, in turn, provides information from the water bottom and can also contain reflections from the water surface.

Depending on the actual incidence angle between laser beam and water surface normal direction, however, it may not be possible to detect an echo from the water surface in either the green or infrared channel. This applies especially to very smooth water surfaces (e.g., an inland lake on a calm day) or to situations where the laser beam hits the side of a water wave front facing away from the sensor. For small-footprint bathymetric sensors in particular, the coaxial emission of both wavelengths is no longer the default. Instead, separate infrared scanners with nadir alignment are used, because the backscattered signal strength from the water surface is particularly high when the laser beams hit the water surface orthogonally due to the mirror-like reflection. Some scanners also do without the infrared channel altogether. In most cases, therefore, refraction correction is based on a gridded 2.5D model of the water surface, which is interpolated from all available surface reflections. While a static water surface can be assumed for standing and running inland waters, the dynamics of the water surface must be taken into account for applications in coastal areas in order to consider wave movements. For the latter, the surface

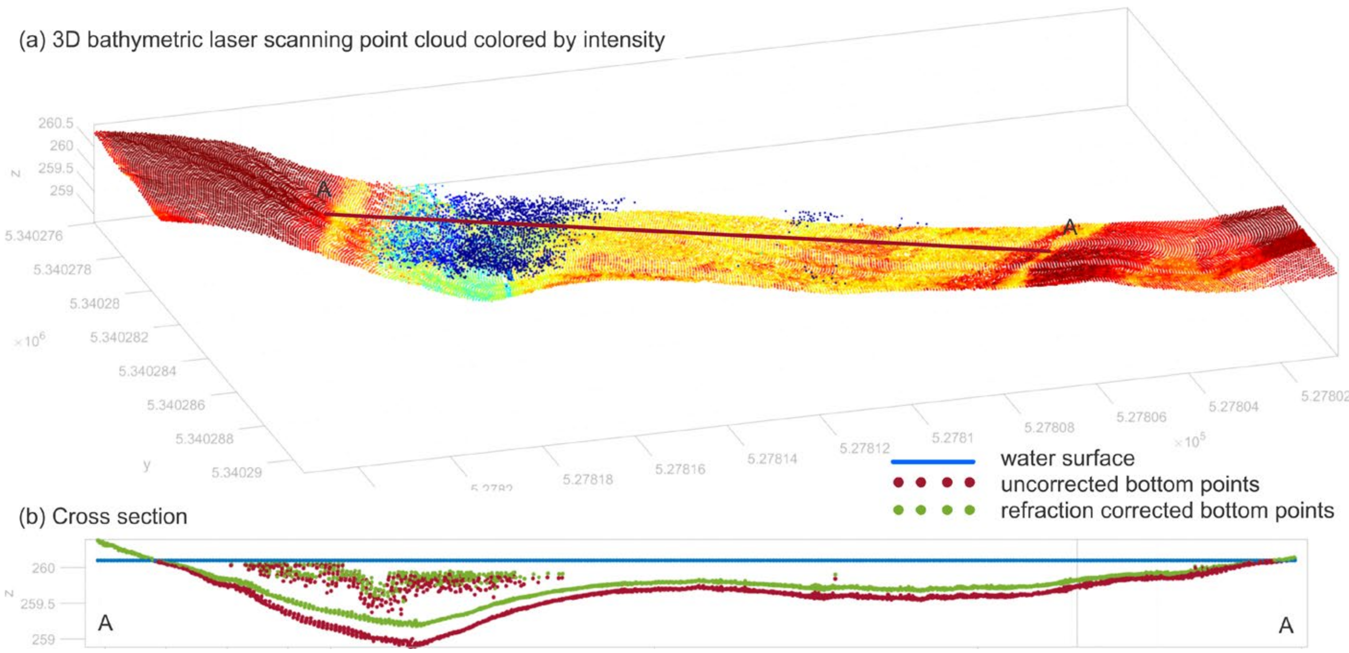


Figure 2: Raw and refraction-corrected bathymetric laser scanning points of a river section. (a) perspective view of raw laser points colored by intensity (red=high, blue = low); (b) cross section showing modeled water surface (blue), raw laser points (red) and refraction-corrected points (green).

model may only be calculated from temporally adjacent laser echoes.

In practice the refraction correction is carried out by applying Snell's law of refraction. For this purpose, the intersection point between the laser beam and the water surface model must first be determined. The laser line is defined by the origin and the beam direction. Ray tracing of the laser line and intersection with the water surface grid model yields the intersection point where the beam is deflected. According to Snell's law of refraction, the water-sided incidence angle ($\alpha_W$) can be calculated from Equation 1 based on the known air-sided incidence angle $\alpha_L$ and the refractive indices in air and water ($n_L$, $n_W$). The distance traveled within the water column results from the time difference between the total travel time and the travel time in the atmosphere. The flight time in the atmosphere is calculated based on the known distance between the origin of the laser and the point of intersection with the water surface, as well as the speed of light in the air. Knowing the reduced propagation speed (group velocity) in water and the direction of the underwater laser ray, refraction-corrected 3D positions of the bottom points can be calculated.

**Figure 2** shows the raw and refraction-corrected points for a short river section. As can be seen from the raw laser points plotted in **Figure 2a** in a perspective view colored by intensity, the point cloud contains seamless points of the river bed and the dry bank area. The intensity of the points decreases with increasing water depth. In addition to the ground points, some points from the water surface and the water column are also recorded, all with relatively low intensity (blue). Note that there is no continuous coverage with water surface points. Especially in the very shallow part of the section, water surface points are missing and extrapolation is necessary to obtain a continuous water surface model. **Figure 2b** shows the modeled water surface (blue) along with the raw (red) and the refraction-corrected (green) water bottom laser points. It is clearly visible that (i) the corrected points are less deep in general due to the slower propagation speed in water and (ii) the amount of the correction scales with water depth.

## Depth penetration and general sensor concepts

In addition to the water's optical properties, the achievable depth of penetration also depends to a large extent on device-specific parameters. The most important influencing factors are the size of the transmitting and receiving optics and their efficiency, the quality of the electronic and electro-optical

| Instrument | ATLAS/ICESat-2 | CZMIL Supernova | HawkEye-5 | CoastalMapper |
|---|---|---|---|---|
| **Manufacturer** | Sigma Space | Teledyne Geospatial | Leica Geosystems | Leica Geosystems |
| **Country** | U.S.A. | Canada | Switzerland/ Sweden | Switzerland/ Sweden |
| **Carrier platform** | satellite | aircraft | aircraft | aircraft |
| **Weight [kg]** | 298 | >300 | ~280 | ~150 |
| **Dimensions [cm]** | n/s | 89 x 60 x 90 | 2x ~ 50 x 50 x 60 | 66 x 59 x 64 |
| **Laser channels [nm]** | 6x 532 | 532/7x 532/1064 | 515/515/1064 | 515/1030/1064 |
| **Camera** | no camera | RGB | RGBI | RGBI |
| **Measurement rate [kHz]** | 10 | 30/210/240 | 40/200/500 | 1000/2000 |
| **Pulse energy [mJ]/ laser class** | 0.2-1.2 | class 4 | n/s | class 4 |
| **Pulse duration [ns]** | 1.5 | 1.65 | n/s | n/s |
| **Field of view [°]** | nadir | 40 | 40 | 50 |
| **Beam divergence [mrad]** | 0.035 | 2/5 | 7.5/4.75/0.5 | 2.75 |
| **Flying altitude [m]** | ~470,000 | 400-800 | 400-600 | 600-900 |
| **Laser footprint [cm]** | 1400 | 75-400 | 190-600 | 165-250 |
| **Scan pattern** | no scanning | circular | elliptical | circular |
| **Depth performance [SD]** | 1 | 2/3 | 2/2.5 | 2.2 |
| **Detection technology** | single-photon | full waveform | full waveform | full waveform |

**Table 1:** Key parameters of spaceborne, airborne and UAV-borne topobathymetric laser scanners.

components (e.g., receiving diodes, A/D converters) and the transmitted laser power. Sensor manufacturers specify the performance of a bathymetric laser scanner as factors related to either the Secchi depth or the diffuse attenuation coefficient *k*. The Secchi depth (SD), named after the 19th century Italian priest and astronomer Angelo Secchi, is an empirical measure that characterizes water turbidity and denotes the water depth at which a white or black-and-white disc with a diameter of 20–30 cm is no longer visible to the naked eye.

Typical SDs are 10–25 m for very clear coastal waters, 3–10 m for alpine rivers and lakes with clear water, 0.5–1.5 m for larger rivers with high sediment content or coastal areas with strong currents (e.g., North Sea). Depending on the application, ALB sensors can be roughly divided into two classes. For the measurement of shallow water zones with water depths <10 m, systems with short pulse lengths (1-2 ns), low beam divergence (0.7-2 mrad) and low laser power are used. Short pulse lengths make it possible to distinguish echoes from the water surface and from the ground even in very shallow areas with water depths of ≤20 cm. The relatively low beam divergence (e.g., 1 mrad = diameter of the laser scan spot of 50 cm at an altitude of 500 m) also ensures good horizontal resolution. Typically, such systems have a high measurement frequency (> 100 kHz), but are limited in the maximum achievable penetration depth (1-2 SD) due to the comparatively low laser power. They are referred to as topobathymetric laser scanners because, in addition to measuring water depths, they can also capture the topography of the dry part of the littoral area, enabling a seamless transition between water and land (see **Figure 2**).

In contrast, purely bathymetric sensors aim for a maximum penetration depth. Systems in this class use high-power lasers. The higher energy is achieved mainly by a longer pulse duration (approximately 7 ns). To ensure eye safety, the laser beam is widened. A typical beam divergence of 7 mrad corresponds to a laser scan spot (footprint) diameter of 3.5 m on the water surface

| | VQ-880-GII | VQ-860-G | VQ-840-GL | Navigator | ABS-SR |
|---|---|---|---|---|---|
| | RIEGL LMS | RIEGL LMS | RIEGL LMS | YellowScan | Fraunhofer IPM |
| | Austria | Austria | Austria | France | Germany |
| | aircraft | helicopter | UAV | UAV | UAV |
| | 65 | 18.5 | 10.5 | 3.7 | 2.5 |
| | 45 x 45 x 69 | 47x 28 x 20 | 36 x 28 x 20 | 35 x 16 x 19 | 32 x 18 x 15 |
| | 532/1064 | 532 | 532 | 532 | 532/1064 |
| | RGBI | RGB | RGB | RGB | --- |
| | 700/900 | 50-100 | 50-200 | 20 | 35 |
| | class 3B | class 3B | class 3B | 0.005 / class 3B | class 2M |
| | 1.5 | 1.5 | 1.5 | 0.850 | ~1 |
| | 40 | 40 | 40 | 40 | 30 |
| | 0.7-2.0 | 1-6 | 1-6 | 4 | constant |
| | 600-700 | 150-500 | 50-300 | 50-100 | 15 |
| | 42-140 | 15-300 | 5-180 | 20-40 | 5 |
| | circular | elliptical | elliptical | linear | elliptical |
| | 1.5 | 2.5 | 2.0 | 2.0 | 1.5 |
| | full waveform | full waveform | full waveform | full waveform | full waveform |

from a flying altitude of 500 m. The typical measurement frequencies of around 30-40 kHz are significantly lower than for topobathymetric systems. With such sensors, penetration depths of about 3 SD can be achieved, which corresponds to a depth of about 50 m in very clear water.

For all systems, the achievable penetration depth also depends on the angle of incidence on the water surface. While most of the energy is scattered back from the water surface by specular reflection when the laser beam hits the water orthogonally, an angle of incidence of about 20° has proven to be an optimal compromise for capturing both the water surface and the bottom (see **Figure 1**). For this reason, Palmer scanners producing a circular scan pattern are generally used in laser bathymetry, since each emitted laser beam hits the water surface at an approximately constant angle of incidence.

## Sensors and platforms

Sensors for recording bathymetry alone or topography and bathymetry together are now used on a variety of carrier platforms such as satellites, aircraft, helicopters and UAVs. The ATLAS (Advanced Topographic Laser Altimeter System) sensor aboard the ICESat-2 satellite is an example of a spaceborne laser sensor with bathymetric capabilities. ATLAS uses single-photon lidar technology. Its prime application is capturing the Earth's cryosphere, but as the sensor uses a green laser (λ=532 nm), it also delivers shallow water bathymetry with a moderate penetration capability of around 1 SD. ICESat-2 data are often used as reference for spectrally derived bathymetry based on optical satellite images, for example, Sentinel-2. High-resolution underwater mapping is not possible with this system due to the large laser footprint diameter (14 m) and the missing scanning mechanism.

At the other end of the scale spectrum, UAV-borne laser bathymetry sensors have been commercially available since around 2018. Compact topobathymetric scanners enable the highest possible spatial resolution with laser footprint sizes in the decimeter range and potential point densities up to 100 points/m$^2$ and more. The downside of drone-based acquisition of bathymetry data is the areal coverage,

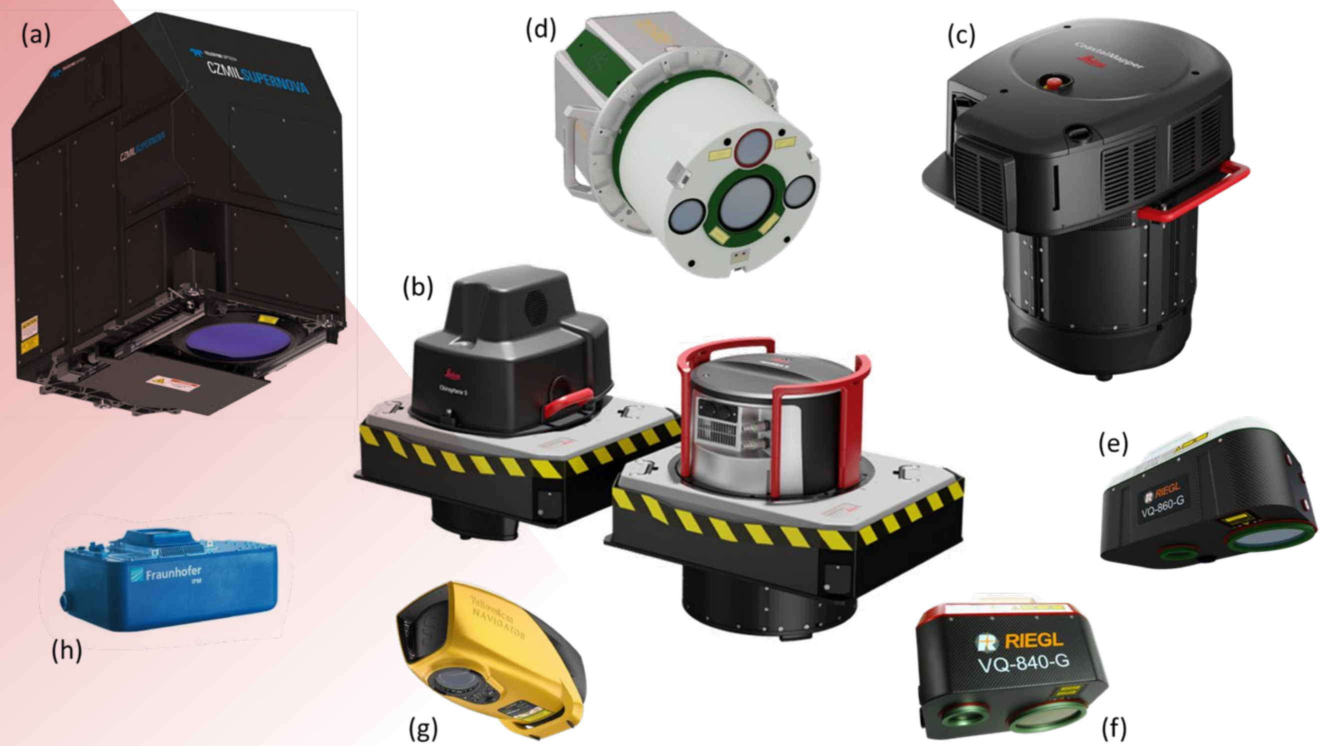


Figure 3: Gallery of commercially available topobathymetric laser scanners: (a) CZMIL SuperNova, (b) HawkEye-5, (c) CoastalMapper, (d) VQ-880-GII, (e) VQ-860-G, (f), VQ-840-GL, (g) Navigator, (h) ABS-SR.

which is limited due to the low flying altitudes and velocities of the drones and their limited flight endurance of approximately 20-30 minutes.

By far the largest group of sensors is operated from either fixed-wing aircraft or helicopters from typical flying altitudes of around 500-750 m. Most manufacturers of survey-grade topographic laser scanners also offer topobathymetric scanners (Teledyne Geospatial, Leica Geosystems, RIEGL Laser Measurement Systems). Scanners carried by aircraft weigh around 30-300 kg and are often equipped with cameras alongside the laser scanners. Some scanners either operate distinct deep channels for maximizing the depth penetration (3 SD) and one or more shallow channels for increasing the spatial resolution (1.5-2.5 SD). Most of the available scanners also provide an infrared (IR) laser channel, either as a separate scanner or in the classical concept with synchronous and coaxial emission with the green laser channel. These systems represent a compromise between good spatial resolution and high area coverage.

**Table 1** summarizes the system parameters of selected state-of-the-art instruments operated from spaceborne, airborne, and UAV-borne platforms. If more than one green channel ($\lambda$=515/532 nm) is reported in **Table 1**, the first refers to the deep and the second to the shallow channel. The measurement rates and laser beam divergences follow the same ordering (green/deep, green/shallow, IR). The resulting laser footprint diameters are reported for the green channels only and mark the range of smallest and largest laser spot sizes considering the sensor's variation of beam divergence and flying altitude. **Figure 3** shows views of the instruments listed in **Table 1**.

CZMIL SuperNova (Teledyne Geospatial) and HawkEye-5 (Leica Geosystems) are examples of sensors equipped with distinct deep and shallow water channels plus an IR channel. CZMIL SuperNova uses a segmented FoV concept, where seven shallow water segments add up to the larger FoV of the deep channel. The instrument enables synchronous and coaxial emission of green and IR laser pulses. The deep channel of the CZMIL sensor has the highest reported penetration depth of 3 SD. The HawkEye-5 sensor

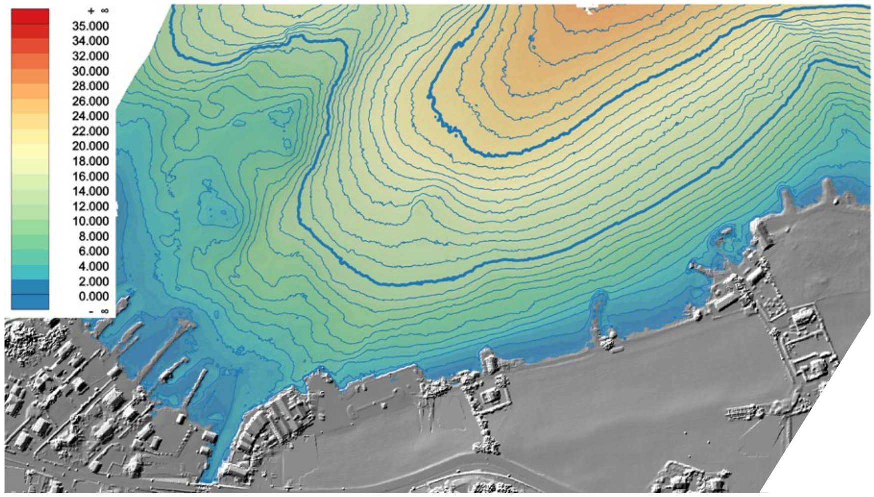


**Figure 4:** DEM hill shading superimposed with color-coded water depth map and depth isolines (isoline intervals 1 and 10 m), derived from Teledyne Optech CZMIL Supernova data

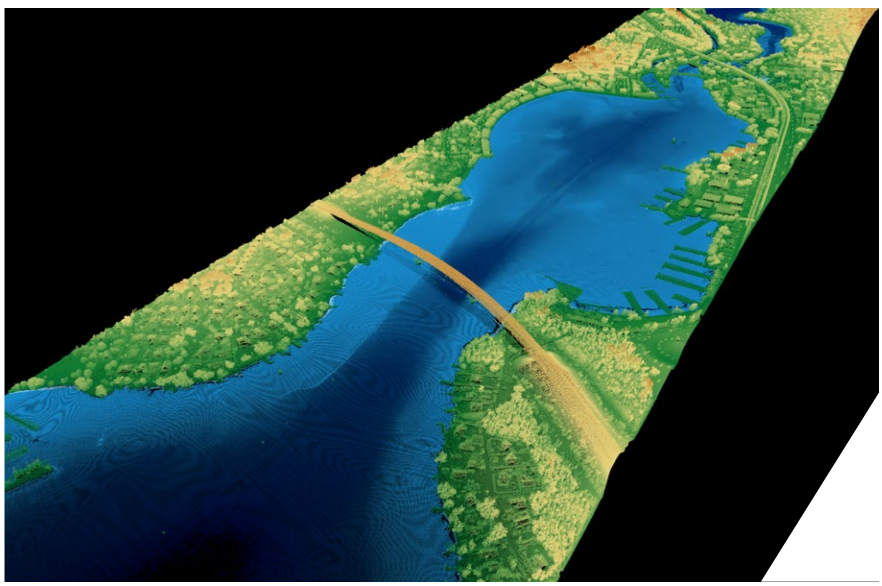

**Figure 5:**: Color-coded 3D point cloud of a flight strip captured with the Leica CoastalMapper sensor.

consists of two separate laser scanners: the HawkEye-5 deep module and the Chiroptera-5 for shallow water. The deep module features a good penetration depth of 2.5 SD at a moderate pulse repetition rate (PRR) of 40 kHz, and the shallow Chiroptera-5 penetrates 2 SD at a PRR of 200 kHz. Leica Geosystems has announced the CoastalMapper, a topobathymetric system consisting of a topographic scanner (Hyperion3) and a newly designed bathymetric scanner (Theia) integrated into a compound sensor head. The scanner maximizes the areal coverage rate for bathymetric surveys by providing a large FoV (50°) and a high flying altitude (800 m).

The VQ-800-G family from RIEGL LMS, in turn, feature the highest resolution of all aircraft- or helicopter based scanners. The VQ-880-GII provides a small laser footprint diameter of 42 cm at the lower flying altitude of 600 m and a high point density due the high pulse repetition rate of 700 kHz for the bathymetric scanner. The VQ-860-G is optimized for helicopter integration with a mass of less than 20 kg and features a user-selectable beam divergence of 1-6 mrad and receiver's FoV (3-18 mrad). This results in a laser spot size of 15 cm when flown at 150 m with the narrowest beam divergence of 1 mrad. The best depth penetration of 2.5 SD, however, is achieved with a low PRR (50 kHz) and wide laser beam (6 mrad). All scanners of the VQ-800-G family have a short pulse duration of around 1.5 ns, which is beneficial for measuring very shallow water depths of around 20 cm.

The intended carrier platform for the VQ-840-GL is a multicopter UAV. The instrument weighs less than 10 kg including GNSS and IMU and can be carried by drones with a maximum take-off-mass (MTOM) of 25-30 kg. With this sensor, very small laser footprints of less than 1 dm and high point densities of >50 points/m$^2$ can be realized when flying slow (e.g., 5 m/s), low (e.g., 50 m) and with a narrow beam (1 mrad). While the VQ-840-G has been available since 2018, more UAV-borne bathymetric laser scanners have emerged more recently. For example, the YellowScan Navigator is a very compact sensor weighing less than 4 kg with a penetration depth of 2 SD at a measurement rate of 20 kHz. This green-only system can be operated at altitudes between 50

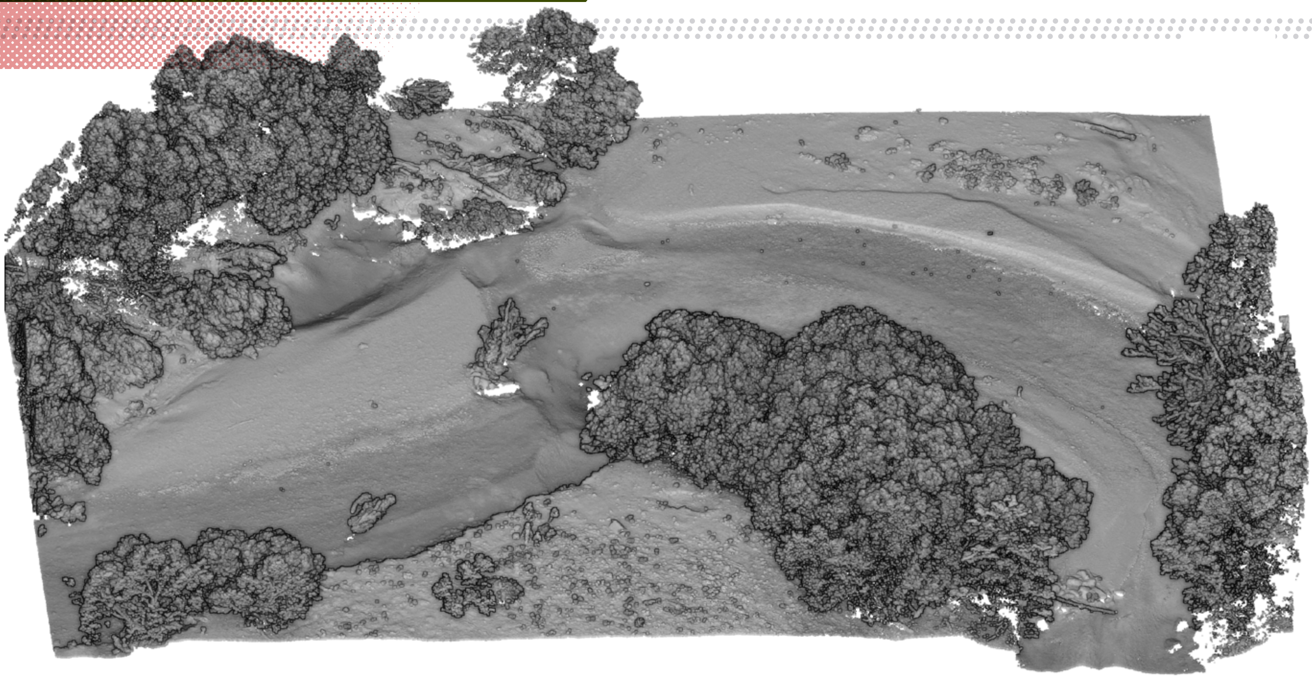

Figure 6: High-resolution point cloud of a section of the Pielach River captured in October 2024 with a RIEGL VQ-840-GL topobathymetric UAV laser scanner.

and 100 m. The short-range Airborne Bathymetric Scanner (ABS-SR) from Fraunhofer IPM is designed for low flight altitudes of 15 m. The scanner synchronously emits green and IR pulses as used in the classic ALB concept. Since the beam widening takes place via lenses in the instrument, the scanner delivers a laser beam with a constant diameter of 5 cm. This makes the sensor particularly interesting for detecting small objects such as underwater vegetation, piles or small boulders.

## Examples of topobathymetric data sets

**Figure 4** shows a DEM hill shading superimposed with a color-coded water depth map and 1 m depth isolines derived from topobathymetric CZMIL SuperNova data (Teledyne Geospatial)[1]. With the deep channel, it was possible to penetrate to a depth of more than 30 m. The topographic channel and the multiple shallow water channels deliver high-resolution topography in the dry-land part of the scene.

**Figure 5** shows a color-coded 3D point cloud of a single flight strip captured with the Leica CoastalMapper sensor. The data was collected during a test flight with a swath width of 800 m and processed with Leica HxMap software. The point cloud shows a seamless transition from water to land and full coverage of topography, vegetation, buildings, and bathymetry[2].

The final example, shown in **Figure 6**, depicts a high-resolution 3D point cloud of a section of the pre-alpine Pielach River in Austria captured in October 2024 with the RIEGL VQ-840-GL topobathymetric UAV laser scanner[3]. Brighter tones in the plot depict higher reflectance. The plot shows all points classified as dry ground, vegetation, and water bottom. For better readability, points classified as water surface, water column, and outliers were discarded. **Figure 6** demonstrates the benefits of the very high spatial resolution (high point density, small laser footprint). For example, occasional small boulders in the riverbed as well as submerged vegetation in the middle of the river can clearly be identified in the point cloud. This opens a path to detailed hydrodynamic-numerical modeling and habitat mapping.

## Selected applications

The range of ALB applications is broad and continually expanding, driven by advances in sensor versatility and miniaturization. Key applications include:

- Underwater object detection: ALB was originally developed for military use in detecting submerged objects. Today, it is widely applied in civil maritime operations, including

1 The data was collected during a calibration flight near the island of Fjøløy (Stavanger, Norway) and kindly provided by the company Field.

2 The image was kindly provided by Leica Geosystems.

3 The data of this example is available as open research data (DOI: 10.48436/taz19-r6618).

harbor security, safe navigation of autonomous underwater vehicles, and monitoring of coastal safety. The detection of small objects requires advanced waveform analysis techniques. The use of UAV-borne ALB has further improved resolution, allowing for the identification of features such as boulders or man-made debris.

- 3D Mapping of submerged topography: Mapping underwater terrain remains the primary use of ALB. It is crucial for creating accurate nautical charts, particularly in shallow coastal and harbor areas. Advances in technology have improved depth penetration, and even satellite-based systems now contribute to near-shore bathymetry. For smaller inland water bodies such as rivers and lakes, high-resolution topobathymetric sensors mounted on crewed or remotely piloted platforms provide the necessary detail. In addition, ALB data is increasingly being integrated systematically into national and regional mapping efforts.
- Ecological applications: ALB supports environmental monitoring in both coastal zones and inland water bodies. It is used to estimate seafloor reflectance and to detect, classify, and model benthic habitats. These capabilities are valuable for habitat conservation and management, as well as for river restoration projects. The ecological relevance of ALB continues to grow, especially in the context of international environmental directives and frameworks.
- Coastal and fluvial geomorphology: ALB is used to analyze both long-term changes and short-term dynamics, such as those induced by hydropeaking. Its high spatial resolution makes it a valuable tool for studying erosion, sediment transport, and river morphology. ALB data also forms the basis for hydrodynamic and flow simulations, supporting a variety of water-related engineering and environmental applications.
- Turbidity estimation: Though turbidity limits the depth to which ALB can penetrate, it also represents a valuable environmental parameter. ALB systems, especially those capable of full-waveform analysis, can be used to estimate water turbidity and assess water quality, supporting ongoing monitoring efforts.
- Risk assessment and disaster management: As extreme weather events become more frequent due to climate change, timely and detailed mapping of coastal and floodplain areas is critical. ALB contributes to both pre- and post-event assessments, offering valuable data for disaster preparedness, response, and recovery. It complements other remote sensing and in-situ measurement methods in comprehensive risk management strategies.
- Macrophyte detection and mapping: We are facing rapid changes in the structure and composition of underwater vegetation, accelerated by climate change. Detection, mapping and monitoring requires the use of high-resolution sensors and agile platforms operating from low altitudes. UAV-based laser scanners are the ideal solution. Their concepts and applications are the focus of the fourth and final part of the airborne lidar tutorial.

**Dr. Gottfried Mandlburger** studied geodesy at TU Wien, where he also received his PhD in 2006 and habilitated in photogrammetry with a thesis on "Bathymetry from active and passive photogrammetry" in 2021. In April 2024 he was appointed University Professor for Optical Bathymetry at TU Wien.

His main research areas are airborne topographic and bathymetric lidar from crewed and uncrewed platforms, multimedia photogrammetry, bathymetry from multispectral images, and scientific software development. Gottfried Mandlburger is chair of the lidar working group of Deutsche Gesellschaft für Photogrammetrie, Fernerkundung und Geoinformation e.V. (DGPF) and Austria's scientific delegate in EuroSDR. He received best paper awards from ISPRS and ASPRS for publications on bathymetry from active and passive photogrammetry.

## Further reading

Abdallah, H., N. Baghdadi et al., 2012. WaLiD. A new lidar simulator for waters, *IEEE Geoscience Remote Sensing Letters,* DOI: 10.1109/LGRS.2011.2180506.

Guenther, G., A. Cunningham, P. Laroque and D. Reid, 2000. Meeting the accuracy challenge in airborne lidar bathymetry, *Proceedings of the 20th EARSeL Symposium: Workshop on Lidar Remote Sensing of Land and Sea,* Dresden, Germany.

Mandlburger, G., 2020. A review of airborne laser bathymetry for mapping of inland and coastal waters, *Journal of Applied Hydrography*, 116: 6–15.

Parrish, C.E., L.A. Magruder et al., 2019. Validation of ICESat-2 ATLAS bathymetry and analysis of ATLAS's bathymetric mapping performance, *Remote Sensing*, DOI: 10.3390/rs11141634.

Philpot, W. (ed.), 2019. *Airborne Laser Hydrography II*, Cornell University Library (eCommons), Cornell. https://ecommons.cornell.edu/handle/1813/66666.

# From Alcatraz to the Maya to Notre-Dame Cathedral and Beyond

## Lidar and 3D technology deliver benefits to discovery, restoration and preservation

Phoenix LiDAR Systems RANGER-U120 ready to fly a mission on Alcatraz Island. The RIEGL VUX-120 lidar sensor on which the system is based is clearly visible.

From preserving the fine details of historical landmarks to uncovering the genius and resourcefulness of ancient civilizations, lidar and 3D rendering technology offer an incredible opportunity to understand humanity's past and present. With geospatial tools and multi-industry collaboration the past can be revealed and the future shaped with more beneficial insights. Recent newsworthy restoration projects such as the Notre-Dame Cathedral, as well as examples from Alcatraz, the Maya, and beyond, show how these cutting-edge technologies provide a fuller picture of the past and help stabilize and modernize for centuries to come.

BY WALTER LAPPERT

### Alcatraz Island

The Alcatraz lidar project in California combined both UAV-lidar and terrestrial laser scanning to capture the entire island, from its rugged coastline to its deteriorating structures, which had served as maximum security federal penitentiary, military prison, and fort. Using the Phoenix RANGER-U120 system, data was collected to produce high-density point clouds of smaller scan areas, capturing details as fine as hairline cracks in the prison cellhouse walls. The resulting dataset provided engineers and preservationists with unprecedented accuracy to assess structural vulnerabilities and prioritize restoration efforts.

The analysis of foundation shifts caused by coastal erosion provided a critical insight. The scan revealed micro-distortions that were invisible to the naked eye but essential to understanding long-term stability risks. By combining


# 3D UNDERWATER MAPPING FROM ABOVE AND BELOW

# WORKSHOP

JOIN US IN VIENNA FOR THE 3RD EDITION OF THE INTERNATIONAL WORKSHOP ON UNDERWATER 3D MAPPING!

**KEY TOPICS** LASER BATHYMETRY | PHOTOGRAMMETRY | 3D MODELING | VR/AR APPLICATIONS | UNDERWATER INFRASTRUCTURE MONITORING | CULTURAL HERITAGE AND ARCHAEOLOGY | HYDROBIOLOGY AND ECOHYDRAULICS | AUTONOMOUS UNDERWATER VEHICLES | SENSOR INTEGRATION AND DATA FUSION | …

## HIGHLIGHTS

- HANDS-ON TUTORIALS
- TECHNICAL SESSIONS
- LIVE DEMONSTRATIONS AT TU WIEN'S WATER LAB FACILITY
- EXCURSION TO PRE-ALPINE PIELACH RIVER
- ALL SOCIAL EVENTS INCLUDED

**SPONSORS:**

## REGISTER NOW

www.conftool.com/3d-underwater2025

UNTIL 22 JUNE 2025

REGULAR: 400€

STUDENT: 350€

FOR INQUIRIES, CONTACT:

3d-underwater@geo.tuwien.ac.at

www.tuwien.at/en/mg/geo/photo/events/3d-underwater


This close-up of the Phoenix LiDAR Systems RANGER-U120 mounted below the UAV shows the Phoenix LiDAR A6K-Lite camera, which acquires high-quality 24.7-megapixel RGB images.

these scans with environmental monitoring data, engineers developed a predictive model to plan for proactive interventions.

Beyond its technical contributions, the Alcatraz project serves a public purpose. The high-resolution 3D data has been incorporated into virtual tours, providing visitors with unparalleled access to areas of the island that are typically off limits. In doing so, lidar has ensured that the story of Alcatraz can be experienced and appreciated by audiences worldwide, preserving not just its physical form but its cultural significance.

## Maya Lowlands

While the Alcatraz project demonstrated lidar's value in preservation, its application in Chiapas, Mexico, showed its potential for discovery. The dense jungles of the Maya Lowlands had long concealed evidence of ancient civilizations, but other UAV-mounted sensors from Phoenix LiDAR Systems transformed the landscape into a detailed map of archaeological features.

One of the most striking findings came from Nuevo Canán, where lidar data uncovered an intricate system of channelized fields and terraces. These features revealed how the Maya adapted to their challenging environment, providing new insights into their agricultural and urban planning practices. Similarly, at Paso del Tigre in Oaxaca, the team identified a 35-meter-long dam and water reservoirs, underscoring the sophistication of Mayan systems for water management.

Processing the data was as critical as collecting it. Ground-classification algorithms filtered out dense vegetation, isolating terrain data and enabling us to detect subtle features like low mounds and terraces. Digital elevation models (DEMs) were enhanced using slope analysis and multi-directional hillshading to visualize anthropogenic modifications. The iterative process of refining the data—balancing automation with manual corrections—ensured that we could confidently distinguish archaeological features from natural topography.

The discoveries in Chiapas not only enhanced our knowledge about the Mayan civilization but also highlighted the potential for lidar to reveal lost histories in other regions of the world.

Lidar's true power lies in its ability to connect the past with the future. In Chiapas, the insights gained from ancient Mayan agricultural techniques could inspire modern approaches to sustainable land use and water management. At Alcatraz, lidar's millimeter-level accuracy has ensured that preservation efforts are guided by data-driven decisions, setting a standard for maintaining historical landmarks in the face of environmental challenges.

> Whether stabilizing a crumbling landmark or revealing an ancient civilization's resilience, lidar reminds us that every structure, every landscape, and every artifact carries a story.

## Notre-Dame Cathedral

A similar story unfolded with the Notre-Dame Cathedral in Paris. Lidar scans from before the catastrophic fire in April 2019 provided the blueprint for its restoration, enabling teams to recreate its intricate Gothic architecture features while addressing structural vulnerabilities. These examples illustrate how lidar doesn't just document history—it informs the strategies needed to ensure that history endures.

## Methodologies and collaboration matter

The success of these lidar and modeling technology projects rests on the precision and adaptability of the methodologies used. At Alcatraz, integrating aerial and terrestrial lidar systems allowed the team to capture the island's varied terrain and structures in exceptional detail. Processing the point clouds involved multiple layers of filtering to eliminate noise and refine the data.

For archaeological projects such as those in Chiapas, additional challenges arose. Dense vegetation and steep terrain required aggressive ground-classification techniques, using advanced software such as LAStools and ArcGIS Pro. Features like defensive walls and reservoirs were made visible through multi-resolution filtering and derivative visualizations such as slope maps and aspect models. This combination of tools and techniques ensured that even subtle features were accurately captured and interpreted.

Lidar's effectiveness depends not only on the technology itself but on the collaboration it fosters. At Alcatraz, the project brought together engineers, conservationists, and historians, each contributing their expertise to interpret the data and implement solutions. In Chiapas, local communities played a vital role in contextualizing the findings, adding cultural depth to the technical data.

This collaborative spirit extends to public engagement. By transforming lidar data into interactive 3D models and virtual experiences, these projects have reached beyond academic and professional circles, inspiring broader awareness and appreciation of cultural heritage.

Lidar has proven itself to be more than just a tool for discovery. It is a means of storytelling, a way to bridge the gap between the worlds we've inherited and the futures we hope to create. From preserving the architectural details of Alcatraz to uncovering the agricultural ingenuity of the Maya, lidar technology offers a lens through which we can better understand humanity's journey.

As the application of lidar continues to expand, so do the possibilities. Whether stabilizing a crumbling landmark or revealing an ancient civilization's resilience, lidar reminds us that every structure, every landscape, and every artifact carries a story. It is up to us to ensure that those stories endure—not just in archives, but in the physical and virtual spaces we share with the world.

---


**Walter Lappert** is a seasoned engineering leader and innovator with extensive expertise in lidar, sonar, radar, GNSS, and photogrammetry technologies. Over his career, he has developed and deployed advanced remote sensing platforms for aerial, terrestrial, and hydrographic data collection, contributing to groundbreaking projects in reality capture, digital twins, and 3D modeling. Currently serving as the Director of Reality Capture at Allen3D, Walter leads cutting-edge initiatives, develops systems, and spearheads innovative applications that harness lidar and 3D rendering technologies to uncover ancient civilizations, modernize historical preservation efforts, and pioneer advances in urban planning.

In addition to his technical contributions, Walter has a strong background in standards development and education, having influenced the standards of the Federal Aviation Administration and the American Society for Testing and Materials for small, unmanned aircraft systems and designed a drone program curriculum for universities. His ability to bridge technology with strategic vision makes him a key figure in leveraging geospatial tools to illuminate the past and shape the future.

# Overview of the ASPRS Positional Accuracy Standards for Digital Geospatial Data

Edition 2, Version 2 (2024)

## ASPRS journey in standards development

The global geospatial community relies on the American Society for Photogrammetry and Remote Sensing (ASPRS) when it comes to education and standardization. Since the early 1980s, ASPRS championed the development of accuracy standards for geospatial data. Early versions, including the legacy standards of 1990, were designed for the map-making practices of that era and characterized by paper-based maps. In 2014, ASPRS published the new Positional Accuracy Standards for Digital Geospatial Data, which were developed for the new digital era of mapping practices. These reflected the vast experience gained from decades of mapping practices and industry use of legacy ASPRS standards. Challenges arose, however, as past experiences were based on older practices and the attendant technology of geospatial data production, which may or may not apply to today's digital sensors, such as lidar and digital cameras. This paper will provide users of the new standards—specifically Edition 2, Version 2 (published on June 24, 2024)—with the necessary details to better understand and apply new accuracy standards in their day-to-day activities.

> "The new standards were designed to be sensor-agnostic and data-driven. Geospatial data users should not worry about data acquisition hardware."

## Design philosophy and the new paradigm

The new standards are intended to be broadly based, technologically independent, and applicable to most common mapping applications and projects. They were developed to embrace the new era of geospatial data acquisition technologies and processing methods. This new direction became apparent when we moved to digital sensors (e.g., lidar and digital cameras) and the resultant digital workflow required to process the acquired digital data. The introduction of digital sensors to our industry put an end to the old concepts of producing and representing map content. The previous era of geospatial

BY QASSIM ABDULLAH

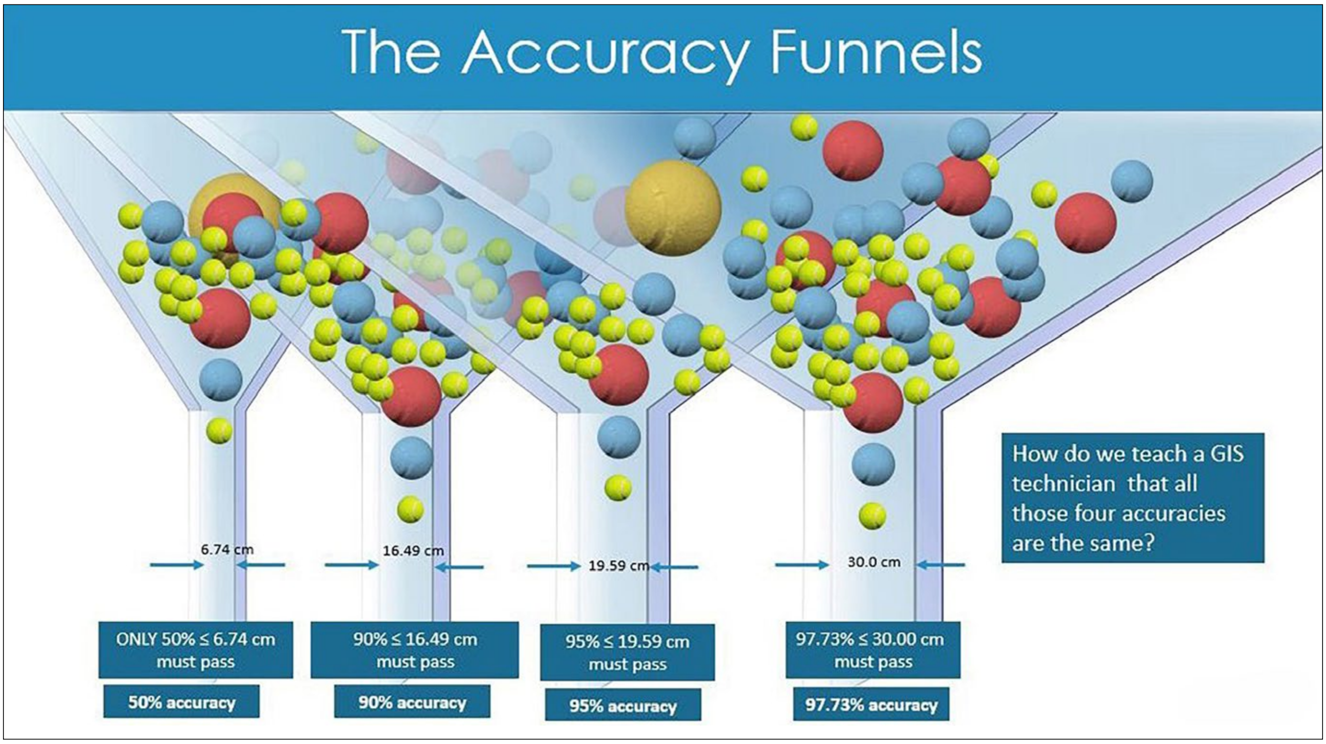


**Figure 1:** The accuracy funnel and statistical concepts.

data production dictated the use of paper as the only medium to present mapping data and the use of map scale and contour interval as measures to represent map accuracy. These legacy accuracy measures were based on the sensor's configuration and other acquisition parameters, such as flying altitude and base-to-height ratio (B/H ratio).

This approach worked for that era because the film camera was the only sensor used to collect data for geospatial data production. Film cameras had a design based on a film format of 220 mm x 220 mm (9 inches x 9 inches) and 150-mm (6-inch) lens focal length. The unique geometrical design made it easy to estimate product accuracy based on flight parameters. Today's digital cameras come with various designs that make it difficult to relate resulting accuracy to the flight parameters. Today's digital geospatial data workflow eliminates the use of these old accuracy measures. The new ASPRS standards were designed to be sensor-agnostic and data-driven. The new paradigm is founded on the fact that geospatial data users should not worry about data acquisition hardware, as it is rapidly changing in response to advances in sensor technologies. Moreover, users should be concerned only about the accuracy of the products they receive and be able to specify product accuracy to suit their project needs. This is what shaped the design philosophy of the new standards. It offers users unlimited accuracy levels without sensor or hardware limitations.

These standards are intended to be a living document to be updated in future editions to reflect changing technologies and user needs.

## Accuracy explained

Historically, geospatial accuracy takes two forms. Firstly, "absolute" accuracy quantifies how close the measured position on a map or in a dataset is to the true physical position, as represented in a reference datum. The other type of accuracy quantifies the internal data quality to express how points within the data relate to each other. Older versions of the ASPRS standards called the latter "relative" accuracy. However, the latest version of these standards changed the term to "data internal precision," as there is wide belief that such measures of data quality do not fall under data accuracy. Accordingly, all references to "accuracy" in the new ASPRS standards and this paper refer to absolute accuracy.

### Adopted statistical measures

The new standards embrace the use of the root mean square error (RMSE) as the only accuracy measure. This is a departure from the earlier version of the standards, Edition 1, where both RMSE and 95% confidence level were used to express product accuracy. The main reason behind this change is to eliminate user confusion experienced since the release of Edition 1 of the standards. Experience showed that only users versed in the probability and statistical theories understood that accuracy expressed in both RMSE and 95% confidence level were the same, the only difference being the confidence levels assigned with each statistical term.

To help readers understand this argument, I would like to describe the differences and similarities in these accuracy terms using the funnel approach. In **Figure 1**, the colored balls represent the errors resulting from an accuracy assessment session using independent checkpoints. The varying ball diameters represent the different values of errors found for each of the checkpoints. The spout diameter of the funnel represents the maximum error value that each of the statistical terms (50%, 90%, 95%, and 97.73%) allows. In **Figure 1**, the largest error allowed is by funnel D, which represents the 97.73% confidence level, while funnel A, which represents a confidence level of 50%, allows the smallest error value of 6.74 cm. If such numbers are presented to an end-user of geospatial data who is unfamiliar with these statistical terms, and you ask the user which accuracy term they prefer, most likely they would choose the smallest number of 6.74 cm, which is represented by funnel A or the 50% confidence level. This choice makes sense for users who prefer the highest

> "Users should be concerned only about the accuracy of the products they receive and be able to specify product accuracy to suit their project needs."

accuracy level they can get for their received products.

If we pose a similar question to those on the product production side, they most likely will choose funnel D, thinking that the larger accuracy number of 30 cm will give some leeway during production. However, both choices based on the accuracy number are wrong, as both the 6.74 cm and 30 cm numbers represent the same accuracy level. Although the 6.74 cm accuracy figure associated with the 50% confidence level is a tight number, only 50% of the balls need to pass through the narrow spout of the funnel. In other words, only 50% of the checkpoints must show an error of 6.74 cm or less. Similarly, 30 cm may look like a looser accuracy figure, but it requires that 97.73% of these balls need to pass through the wide spout of the funnel. In other words, 97.73% of the checkpoints must have an error of no larger than 30 cm. As you may notice, it becomes very confusing for the layperson to notice and understand all these details. That is why we removed the 95% confidence level—it offers no additional benefits over RMSE, while causing considerable confusion.

### The 3D accuracy approach

The new standards introduce yet another accuracy term for the new era of engineering and geospatial needs—three-dimensional accuracy. When considering the fast pace of development in the field of digital twins, smart cities, and other applications that require three-dimensional representation of features, we wanted to offer a way to measure feature accuracy within a three-dimensional model. Currently, we estimate horizontal and vertical accuracy separately, which is helpful in describing the accuracy of 3D models. However, it is not as efficient for representing accuracy in the native 3D environment.

### Horizontal positional accuracy standard for geospatial data

Horizontal accuracy is meant for products that live in a two-dimensional space, such as a planimetric map or an ortho map. In practice, geospatial data users pay less attention to feature vertical accuracy in products such as flat maps, because there is no way to measure the height or model the vertical accuracy. The new standards offer a simple yet comprehensive approach for horizontal accuracy. They offer unlimited horizontal accuracy classes to suit any geospatial product and make it useful over time regardless of changes in future technologies or practices.

**Table 1** presents the horizontal accuracy standards of the new standards. The accuracy class is determined by the user or by project needs. Once the user specifies that their project requires, for example, an accuracy of 5 cm, that figure becomes the accuracy class according to the new ASPRS standard. Consequently, 5 cm will be interpreted as the absolute horizontal accuracy measured as RMSE. Additionally, the horizontal accuracy standards set an accuracy measure for the mosaic seamlines mismatch. Before the advanced digital image processing tools and efficient matching algorithms, users struggled to stitch images (or frames) together without visible shifts in features, such as roads and buildings, extending over adjacent frames. Because it was impossible to eliminate a mismatch between frames, the industry (and therefore accuracy standards) accepted some mismatch, within a certain tolerance. This tolerance is provided in **Table 1**.

Today's image processing is more refined and rarely are users faced with these issues. Although it is uncommon, edge mismatch may still occur in some projects that were either poorly collected or processed, or if an inaccurate digital elevation model (DEM) was used during orthorectification.

| Horizontal Accuracy Class | Absolute Accuracy $RMSE_H$ (cm) | Orthoimagery Mosaic Seamline Mismatch (cm) |
|---|---|---|
| # cm | ≤ # | ≤ 2*# |

Table 1: Horizontal accuracy classes for geospatial data.

To assess the horizontal accuracy for an orthorectified map, for example, a minimum of 30 independent checkpoints clearly visible on the map should be surveyed to an accuracy that suits the expected map accuracy.

## Vertical positional accuracy standard for elevation data

Like horizontal accuracy standards, vertical accuracy standards offer a simple but comprehensive approach for all geospatial products (**Table 2**). Different from horizontal accuracy standards, vertical accuracy standards include two categories for vegetated and non-vegetated terrains. However, the non-vegetated vertical accuracy (NVA) is the one that will be considered when accepting or rejecting data based on the results of the vertical accuracy assessment. The vegetated vertical accuracy (VVA) has no threshold and should be assessed and reported as found, with no weight on accepting or rejecting the data unless there is a different prior agreement reached between the data user and the data producer. If the user specifies a 10-cm vertical accuracy requirement for their product, this will go on the record as a 10-cm vertical accuracy class as NVA with $RMSE_V$ = 10 cm.

NVA should be assessed using a minimum of 30 independent checkpoints and up to 120 checkpoints for large projects. The VVA needs a minimum of 30 checkpoints regardless of the project size unless otherwise agreed upon between the data user and the data producer. The vertical accuracy standards also introduce measures for data internal precision such as within-swath data smoothness and vertical shift in data from adjacent swaths. Here you notice that standards refrain from using the term "relative accuracy" and replace it with the new term "data internal precision", as data smoothness does not fall under accuracy. In lidar, for example, data smoothness is mainly related to the hardware performance and does not follow the theories of statistics and probability like absolute accuracy.

| 3D Accuracy Class | Absolute Accuracy |
|---|---|
| | $RMSE_{3D}$ (cm) |
| # cm | ≤ # |

Table 3: Three-dimensional accuracy classes for geospatial data.

| Vertical Accuracy Class | Absolute Accuracy | | Data Internal Precision (where applicable) | | |
|---|---|---|---|---|---|
| | NVA $RMSE_V$ (cm) | VVA $RMSE_V$ (cm) | Within-Swath Smooth Surface Precision Max Diff (cm) | Swath-to-Swath Non-Vegetated $RMS_{DZ}$ (cm) | Swath-to-Swath Non-Vegetated Max Diff (cm) |
| #-cm | ≤ # | As found | ≤ 0.60*# | ≤ 0.80*# | ≤ 1.60*# |

Table 2: Vertical accuracy classes for digital elevation data.

## Three-dimensional positional accuracy standard for geospatial data

As mentioned earlier, our industry is heading towards a 3D GIS concept. This is evident in the use of colorized point clouds, 3D models, digital twins, etc. Such a 3D environment requires a suitable new accuracy measure. The introduction of a 3D positional accuracy standard as a new accuracy measure is introduced to meet such needs. **Table 3** lists the 3D positional accuracy standard and presents unlimited accuracy classes to suit all application needs.

The one concern to be addressed by the software suppliers is the lack of a commercial viewer for true 3D data visualization and manipulation. The industry needs an application that is easily accessible to all geospatial data users with smooth viewing of the 3D model. Users need an application with a terrain-hugging floating mark or cursor to measure feature position in a true 3D environment. Without such a capability, users currently combine individually assessed vertical and horizontal accuracies to produce 3D accuracy for their products.

## Ground controls and products' accuracy

Surveyed control points play a crucial role in assessing and improving products' absolute accuracy. Whether used to process lidar or digital imagery, the number and distribution of ground control points are determined by expected product accuracy. There is no single method to determine the number and distribution scheme, as the approach is based on practical experience coupled with user judgement. The general rule, however, is that ground control points and checkpoints should be evenly distributed throughout the project area unless there are natural factors (such as water and heavy vegetation) that may prevent or skew such distribution. As for the quality of the surveyed control points, these standards require that the survey meets specific accuracy criteria to produce the final mapping products from these points. Survey accuracy requirements differ according to mapping product type, i.e., whether it is two-dimensional (ortho map) or three-dimensional (elevation data). The new standards set the following requirements for ground control points for imagery-based products:

- Ground control for aerial triangulation designed for digital planimetric data (orthoimagery and/or map) only:
  - $RMSE_{H(GCP)} \leq ½ *RMSE_{H(MAP)}$
  - $RMSE_{V(GCP)} \leq RMSE_{H(MAP)}$
- Ground control for aerial triangulation designed for projects that include elevation or 3D products, in addition to digital planimetric data (orthoimagery and/or map):
  - $RMSE_{H(GCP)} \leq ½ *RMSE_{H(MAP)}$
  - $RMSE_{V(GCP)} \leq ½ *RMSE_{V(DEM)}$
- Similarly, the accuracy of the ground control points used for lidar calibration and boresighting should be twice the target accuracy of the final products.
  - $RMSE_{V(GCP)} \leq ½ *RMSE_{V(DEM)}$
- Currently, the industry is focusing only on the vertical accuracy of lidar datasets. If a horizontal accuracy measure is required for lidar data, users can adopt the one provided for imagery-based products or:
  - $RMSE_{H(GCP)} \leq ½ *RMSE_{V(DEM)}$

## Accuracy assessment

For projects requiring accuracy testing according to ASPRS standards, perform the testing according to the following understanding:

- **Horizontal accuracy**: Compare planimetric coordinates in the data set with those from a more accurate source.
- **Vertical accuracy**: Compare surface elevations in the data set with those from a more accurate source, using checkpoints and scientifically sound interpolation methods.
- **Three-dimensional accuracy**: Compare the combined X, Y, and Z coordinates in the data set with those from a more accurate source.

An unbiased accuracy assessment is the only way geospatial data users can be certain that the delivered products meet project or application requirements. For the assessment to be unbiased, the following conditions must be satisfied:

1. The surveyed checkpoints used in the assessment should be independent of the surveyed control points used in the data calibration process, i.e., assessment checkpoints are not used in the imagery aerial triangulation process or the boresighting of lidar data.
2. The accuracy of the checkpoints should be higher than the expected accuracy of the tested product. According to these standards, the accuracy of the checkpoints should be at least twice as much as the expected accuracy of the tested product.
3. Checkpoints should be evenly distributed around the project as much as feasible. Terrain and

access may affect this distribution, requiring practical judgment to be applied.

4. A minimum of 30 checkpoints should be used for assessing horizontal accuracy and the NVA for project areas of 1000 km$^2$. Such numbers increase with project size (**Table 4**).

If the project cannot meet the 30-checkpoint minimum due to small test area (e.g., UAV-based projects) or budget constraints, report accuracy verification with fewer checkpoints, according to section 7.16 of the standards.

As for assessing VVA, the standards recommend a minimum of 30 checkpoints regardless of the project size. Data users and data producers can agree, however, on additional or fewer checkpoints if this suits the project requirements.

The previously recommended number and distribution of NVA and VVA checkpoints may vary according to the significance of different land cover categories and project requirements. The checkpoint numbers suggested in **Table 4** are recommendations based on best practices. Data producers and data users may mutually agree to modify such requirements based on anticipated accuracy, project area and scope, terrain challenges, accessibility of the area, and budget constraints.

## Accuracy reporting

Horizontal, vertical, and 3D positional accuracies shall be assessed and formally reported according to one of the statements provided in section 7.16 of the standards. In addition to the accuracy class, the following related statistical quantities should be computed and reported:

- Residual errors at each checkpoint
- Maximum error
- Minimum error
- Mean error
- Median error
- Standard deviation
- RMSE.

The standards differentiate when the accuracy is performed by data users versus data producers.

| Project Area (Square Kilometers) | Total Number of Checkpoints for NVA |
|---|---|
| ≤1000 | 30 |
| 1001–2000 | 40 |
| 2001–3000 | 50 |
| 3001–4000 | 60 |
| 4001–5000 | 70 |
| 5001–6000 | 80 |
| 6001–7000 | 90 |
| 7001–8000 | 100 |
| 8001–9000 | 110 |
| 9001–10000 | 120 |
| >10000 | 120 |

Table 4: Checkpoint recommendations for horizontal accuracy and NVA testing based on project area.

## Accuracy reporting by data users or their consultants

The standards provide specific statements to report the three types of positional accuracies. Such statements are specific to whether the accuracy testing meets the ASPRS standards requirement for 30-checkpoint minimum.

## When accuracy testing meets ASPRS standards requirements

Here the testing should be performed using a minimum of 30 checkpoints.

- **Reporting horizontal positional accuracy**
  *"This data set was tested to meet ASPRS Positional Accuracy Standards for Digital Geospatial Data, Edition 2, Version 2 (2024) for a __(cm) RMSE$_H$ Horizontal Positional Accuracy Class. The tested horizontal positional accuracy was found to be RMSE$_H$ = __(cm)."*
- **Reporting NVA**
  *"This data set was tested to meet ASPRS Positional Accuracy Standards for Digital Geospatial Data, Edition 2, Version 2 (2024) for a __(cm) RMSE$_V$ Vertical Accuracy Class. The Non-Vegetated Vertical Accuracy (NVA) was found to be RMSE$_V$ = __(cm)."*
- **Reporting VVA**
  *"This data set was tested to meet ASPRS Positional Accuracy Standards for Digital Geospatial Data, Edition 2, Version 2 (2024) for a __(cm) RMSE$_V$ Vertical Accuracy Class. The Vegetated Vertical Accuracy (VVA) was found to be RMSE$_V$ = __(cm)."*
- **Reporting 3D positional accuracy**
  *"This data set was tested to meet ASPRS Positional Accuracy Standards for Digital Geospatial Data, Edition 2, Version 2 (2024) for a ___ (cm) RMSE$_{3D}$ Three-Dimensional Positional Accuracy*

*Class. The tested three-dimensional accuracy was found to be $RMSE_{3D}$ = ___(cm) within the NVA tested area and $RMSE_{3D}$ = ___(cm) within the VVA tested area."*[1]

## When accuracy testing does not meet ASPRS standards requirements

The following reporting statements are designed for when testing is performed using fewer than 30 checkpoints. This could be due to the small size of the project or low budget. Many UAV projects fall into this category. Although the standards do not endorse the assessed accuracy performed with fewer than 30 checkpoints, they provide a vehicle to report findings regardless and at the same time encourage truth-in-reporting:

- **Reporting horizontal positional accuracy**
  *"This data set was tested as required by ASPRS Positional Accuracy Standards for Digital Geospatial Data, Edition 2, Version 2 (2024). Although the Standards call for a minimum of thirty (30) checkpoints, this test was performed using ONLY __ checkpoints. This data set was produced to meet a ___(cm) $RMSE_H$ Horizontal Positional Accuracy Class. The tested horizontal positional accuracy was found to be $RMSE_H$ = ___(cm) using the reduced number of checkpoints."*
- **Reporting NVA**
  *"This data set was tested as required by ASPRS Positional Accuracy Standards for Digital Geospatial Data, Edition 2, Version 2 (2024). Although the Standards call for a minimum of thirty (30) checkpoints, this test was performed using ONLY __ checkpoints. This data set was produced to meet a ___(cm) $RMSE_V$ Vertical Positional Accuracy Class. The tested vertical positional accuracy was found to be $RMSE_V$ = ___(cm) using the reduced number of checkpoints in the NVA tested area."*
- **Reporting VVA**
  *"This data set was tested as required by ASPRS Positional Accuracy Standards for Digital Geospatial Data, Edition 2, Version 2 (2024). Although the Standards call for a minimum of thirty (30) checkpoints, this test was performed using ONLY __ checkpoints. This data set was produced to meet a ___(cm) $RMSE_V$ Vertical Positional Accuracy Class. The tested vertical positional accuracy was found to be $RMSE_V$ = ___(cm) using the reduced number of checkpoints in the VVA tested area."*
- **Reporting 3D positional accuracy**
  *"This data set was tested as required by ASPRS Positional Accuracy Standards for Digital Geospatial Data, Edition 2, Version 2 (2024). Although the Standards call for a minimum of thirty (30) checkpoints, this test was performed using ONLY __ checkpoints. This data set was produced to meet a ___(cm) $RMSE_{3D}$ Three-Dimensional Positional Accuracy Class. The tested three-dimensional positional accuracy was found to be $RMSE_{3D}$ = ___(cm) using the reduced number of checkpoints in the NVA tested area and $RMSE_{3D}$ = ___(cm) using the reduced number of checkpoints in the VVA tested area."*

## Accuracy reporting by data producers

Data producers do not usually have access to independent checkpoints and, most of the time, they use the ground controls used in aerial triangulation or lidar boresighting to assess product accuracy. Of course, this practice is a biassed test (and therefore unacceptable) because the checkpoints were used in product calibration. Reporting statements by data producers are much simpler, however, as they do not report the accuracy results. They are merely a declaration of what they promised to produce according to the contract requirements. Data producers rely on their vast experience of producing similar products in the past, assuming they employ mature technologies, and follow the best practices and guidelines through established and documented procedures during project design, data processing, and quality control, as set forth in the addenda to these standards.

- **Reporting horizontal positional accuracy**
  *"This data set was produced to meet ASPRS Positional Accuracy Standards for Digital Geospatial Data, Edition 2, Version 2 (2024) for a __(cm) $RMSE_H$ Horizontal Positional Accuracy Class."*
- **Reporting NVA**
  *"This data set was produced to meet ASPRS Positional Accuracy Standards for Digital Geospatial Data, Edition 2, Version 2 (2024) for a __(cm) $RMSE_V$ Non-Vegetated Vertical Accuracy (NVA) Class."*
- **Reporting VVA**
  *"This data set was produced to meet ASPRS Positional Accuracy Standards for Digital Geospatial Data, Edition 2, Version 2 (2024) for*

1 The 3D positional accuracy in vegetated areas can be omitted from this report based on a mutual agreement between the data user and the data producer.

*a __(cm) $RMSE_V$ Vegetated Vertical Accuracy (VVA) Class."*

- **Reporting 3D positional accuracy** *"This data set was produced to meet ASPRS Positional Accuracy Standards for Digital Geospatial Data, Edition 2, Version 2 (2024) for a ___ (cm) $RMSE_{3D}$ Three-Dimensional Positional Accuracy Class within the NVA tested area and $RMSE_{3D}$ = ___(cm) within the VVA tested area."*

## Horizontal accuracy of elevation data

The topic of horizontal accuracy was rarely dealt with before Edition 1 of the ASPRS standards. Among the main reasons for this lack of focus were:

**Horizontal accuracy is difficult to verify in the field:** Whether it is from lidar or imagery, a point cloud is a discrete data set with sparse points, which make it difficult to model a ground feature to accurately recognize it in the field and pinpoint its horizontal accuracy within a few centimeters. An example is a lidar data set produced to meet USGS QL1. The nominal post spacing for QL1 is 35 cm, which does not support measuring horizontal features much smaller than 35 cm. As point cloud density increases with the advance of lidar technology, however, this task is becoming more achievable. Fortunately, the situation for a point cloud produced from imagery is different, because there is more control over producing a very high point-cloud density.

**Horizontal accuracy was not needed:** The previous era of mapping was not focussed on 3D model representation and most applications were designed to produce land contours. In today's world and with the introduction of new concepts such as digital twin, smart city, autonomous driving, indoor scanning and BIM, knowing how accurate the data is horizontally is crucial for public safety and data performance reasons. The introduction of new 3D accuracy in the ASPRS standards is a testimony to these new applications and requirements.

This formula was crossed-checked with horizontal accuracy computation by two of the main manufacturers of aerial lidar systems and resulted in broad agreement.

The above formula simplifies the error budget in lidar and reflects the main contributors to that error budget.

> "Incorporating the field surveying accuracy is now crucial in determining the real product accuracy."

The new standards offer the following approaches for deriving or estimating horizontal accuracy:

- **For photogrammetrically derived elevation data,** adopt the same horizontal accuracy class assigned for planimetric data or digital orthoimagery produced from the same source, based on the same photogrammetric adjustment.
- **For lidar elevation data,** the standards provide the following formula for estimating the horizontal accuracy:

$$RMSE_H = \sqrt{(GNSS\ positional\ error)^2 + \left(\frac{\tan(IMU\ roll\ or\ pitch\ error) + \tan(IMU\ heading\ error)}{1.478} * flying\ height\right)^2}$$

Where:

- Flying height above mean terrain is in meters
- GNSS positional errors are radial, in meters, and can be derived from published manufacturer specifications
- IMU errors are in angular units and can be derived from published manufacturer specifications.

Horizontal error in lidar-derived elevation data is largely a function of the following parameters:

- Sensor positioning error as derived from the Global Navigation Satellite System (GNSS)
- Attitude (angular orientation) error as derived from the IMU
- Flying height above mean terrain.

There are other error sources in the lidar system, such as laser ranging and clock timing, which are ignored by the equation as they contribute minimally to the error budget and are considered negligible when estimating horizontal error. The error caused by laser-beam divergence is also ignored for reasons detailed in section 7.6 of the standards.

## The role of control survey accuracy in product accuracy

Edition 2 of the standards introduces a requirement for considering the survey accuracy of ground control and checkpoints when computing product final accuracy. Today's advances in lidar, digital sensors, and digital analytical modeling enable us to produce highly accurate geospatial products that in some cases exceed the accuracy of the field surveying techniques such as GNSS-based RTK. Incorporating the field surveying accuracy is now crucial in determining the real product accuracy, but was not needed decades ago when sensors and procedures yielded far less accurate products. Therefore, when we're dealing with products such as DOQQ with an accuracy of 10 m, a few centimeters of error in the checkpoints does not impact the final product accuracy.

The new approach introduced by the ASPRS standards divides the product accuracy into two parts or components. The first component includes $RMSE_{H1}$ and $RMSE_{V1}$ error is derived from the product fit to the checkpoints. The second component includes $RMSE_{H2}$ and $RMSE_{V2}$, which represent errors associated with the accuracy of the survey of the checkpoints. Both components are needed to compute the product's final accuracy:

$$Horizontal\ Product\ Accuracy\ (RMSE_H) = \sqrt{{RMSE_{H_1}}^2 + {RMSE_{H_2}}^2}$$

$$Vertical\ Product\ Accuracy\ (RMSE_V) = \sqrt{{RMSE_{V_1}}^2 + {RMSE_{V_2}}^2}$$

$$RMSE_{3D} = \sqrt{{RMSE_H}^2 + {RMSE_V}^2}$$

Such requirements make it obligatory for data users and data producers to be acquainted with the field surveying process through their surveyors. In other words, they ultimately will need to know the accuracy of the survey so they can use it in the previous formulae. Experience reveals that many of the field surveying manufacturers do not provide the absolute accuracy figures needed for these formulae. Instead, several produce quality figures representing data internal precision that should not be used in these formulae. Acknowledging such a problem, the standards provided in **Table 5** comprise a list of the predicted accuracy for most of the surveying techniques used by the industry today. We hope that the manufacturers of surveying equipment recognize the needs of their clients who want to embrace the new ASPRS standards by coming up with a way to compute the absolute accuracy of the survey.

## Vegetated versus non-vegetated accuracy

The new standards introduce an important change to the assessment of accuracy in vegetation. Some vegetated environments are challenging for many aerial data acquisition sensors, such as lidar and imagery. The new standards remove the pass/fail criteria for the VVA and now it needs to be tested and reported according to the requirements outlined in these standards. The logic behind this change is based on the following:

**Lidar (and imagery) cannot penetrate dense vegetation perfectly:** This problem results in a less dense lidar point cloud under trees. A sparse point cloud results in less favorable modeling of the terrain under trees. Due to this compromised modeling of the terrain, the VVA assessment results in a bad fit of the checkpoints to the lidar point cloud. **Figure 2** illustrates the problem in modeling terrain using a sparse point cloud and a dense point cloud. When terrain is modeled with a less dense point cloud, there is a risk of estimating the wrong elevation for the desired location, such as point A of the top profile of **Figure 2**. The software used most likely creates a triangulated irregular network (TIN), whereby connections between points of the point cloud form triangles. Software reports terrain elevation at a certain location based on linear interpolation inside the triangle within which the location falls.

As depicted in **Figure 2**, due to the sparse point cloud around point A, its elevation could be estimated with an error of 2 m. Point A could be one of the checkpoints surveyed under trees to assess VVA. When this happens, the derived VVA cannot be trusted. The only way to prevent such errors is by having a smooth continuous model to represent the terrain, which can be guaranteed only by having a dense point cloud to model the terrain accurately, as illustrated in the lower surface of **Figure 2**. More details on this topic can be found in section D of addendum I of the standards.

**Surveying under trees is not reliable:** GPS signals and PDOP are disturbed under dense canopies, resulting in inaccurate surveys.

**Field survey measures the actual ground:** The survey team usually measures the elevation of the actual ground, while the lidar point cloud measures the tops of the leaves, debris, and grass overlaying the ground. Such discrepancies in the measured elevations undermine the assessed VVA.

**The forest floor is dynamic in nature:** Forest floor debris moves with wind, water runoff, and animals disturbing the soil. In addition to the error vegetation already introduces, it changes in height and shape over time, which can pose serious problems, especially if the field ground survey is not performed at the same time as the airborne survey.

**The advanced sensor technology on the market produces highly accurate point clouds:** It is therefore appropriate to base data acceptance or rejection on the accuracy of the data over bare earth, where the ground is not obscured from the sensor. This was done for decades in photogrammetry, when under-tree area contours were drawn as dash contours to indicate a low-confidence area where accuracy was not guaranteed.

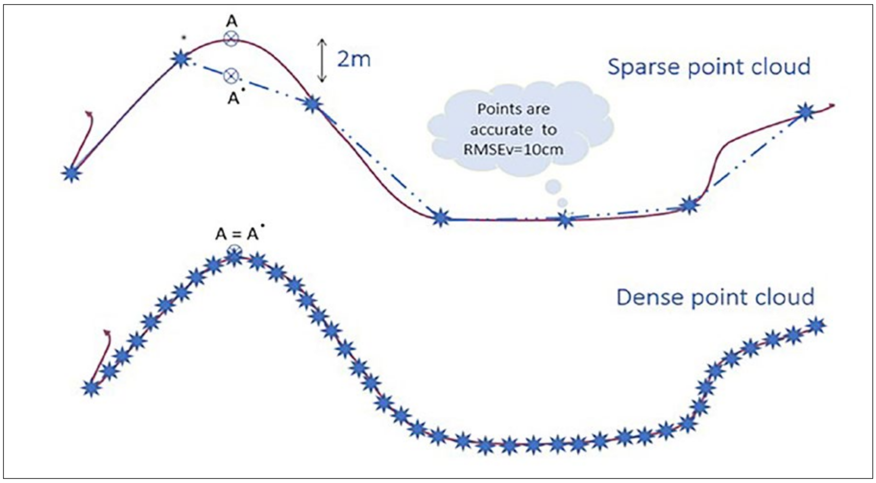

Figure 2: Terrain modeling quality as a function of point density and vertical accuracy.

| Survey Methodology | Predicted Accuracy Values | | |
|---|---|---|---|
| | Horizontal | Vertical | 3D |
| Adjusted Closed Loop–Digital Leveling | | 5 mm | |
| Real-Time Network Following Section C–Recommended Procedures | 10 mm | 16 mm | 19 mm |
| Real-Time PPP After Convergence Following Section D–Recommended Procedures | 15 mm | 24 mm | 28 mm |
| Real-Time Kinematic (RTK) Base and Rover Following Section B–Recommended Procedures | 20 mm | 32 mm | 38 mm |
| Closed Conventional Traverse Following Section E–Recommended Procedures | 25 mm | 40 mm | 47 mm |
| Real-Time PPP After Convergence, Single Measurement | 20 mm | 50 mm | 54 mm |

Table 5: Predicted accuracies of field surveying techniques.

## The power of the six addenda

For the first time, ASPRS standards contain best practices and guidelines for use. The information included in these addenda is not easily found in a textbook or a technical paper. It is a collection of science and practical experience authored by professionals with decades of surveying and mapping practice. The following is a brief description of these addenda:

### Addendum I: General Best Practices and Guidelines

This addendum provides information on the following topics:

- Reporting notes for delivered geospatial products
- Error normality testing and reporting
- Understanding accuracy statistics and errors mitigation
- Lidar data quality versus positional accuracy
- Lidar system classification and grouping.

### Addendum II: Best Practices and Guidelines for Field Surveying for Ground Control Points and Checkpoints

This addendum is a valuable addition which details everything users need to know about conducting safe and successful field surveys. No person should start a survey in the field for projects that must meet ASPRS standards without first consulting this addendum.

### Addendum III: Best Practices and Guidelines for Mapping with Photogrammetry

This addendum walks users through all aspects of photogrammetric mapping, from planning to aerial data collection, production and accuracy assessment. It is a valuable resource for practitioners as well as those just starting their careers in photogrammetric mapping.

**Addendum IV: Best Practices and Guidelines for Mapping with Lidar**
Lidar is becoming the backbone of our industry and the money-maker for almost all mapping businesses. This addendum provides information similar to that provided in addendum III for photogrammetric mapping but with a focus on lidar, lidar sensors, and operations.

**Addendum V: Best Practices and Guidelines for Mapping with Unmanned Aerial Systems (UAS)**
While UAS is taking our industry and other aspects of life by storm, this addendum provides everything needed to create a successful production line for UAS operations. It contains two sections—one focused on photogrammetric operations and production and the other on UAS-based lidar operations and production.

**Addendum VI: Best Practices and Guidelines for Mapping with Oblique Imagery**
The market lacks good information about best practices in oblique imagery operations. That was the motive behind drafting this addendum, which contains information about acquisition and production of oblique imagery that is difficult to find anywhere else.

## Acknowledgments

The author and ASPRS deeply appreciate the many volunteers who dedicated two years of their time to create Edition 2, Version 2. Their names are listed on the back of the published standards. We are forever grateful for their efforts and generosity.

This article will be published concurrently in *Photogrammetric Engineering & Remote Sensing* and *LIDAR Magazine*.

Woolpert Vice President and Chief Scientist **Qassim Abdullah, PhD, PLS, CP**, has more than 45 years of combined industrial, R&D, and academic experience in analytical photogrammetry, digital remote sensing, and civil and surveying engineering. When he's not presenting at geospatial conferences around the world, Abdullah teaches photogrammetry and remote sensing courses at the University of Maryland and Penn State, authors a monthly column for the ASPRS journal *Photogrammetric Engineering & Remote Sensing*, sits on NOAA's Hydrographic Services Review Panel, and mentors R&D activities within Woolpert and around the world.

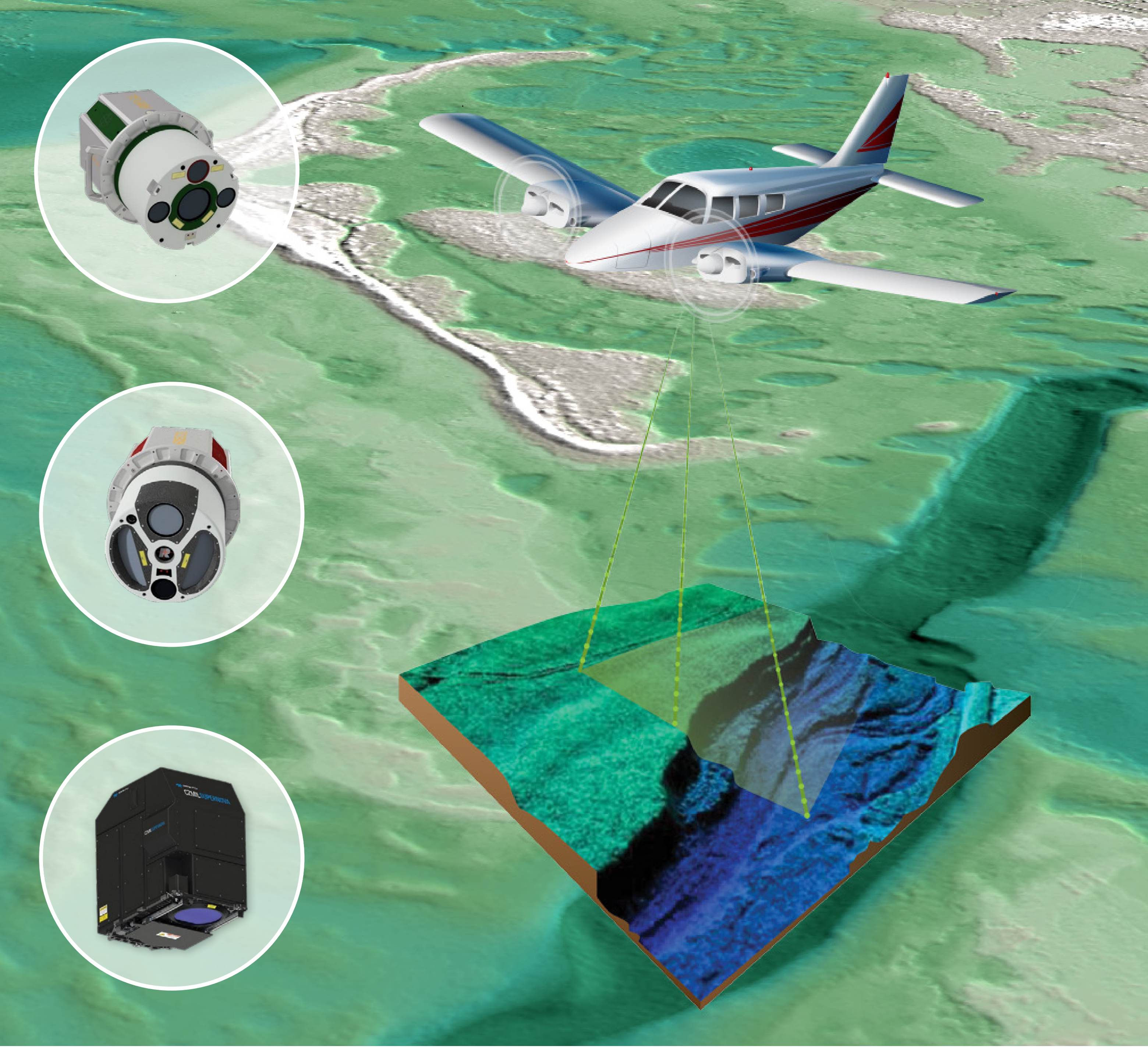

***Walker,*** *continued from page 48*

Maune's military career continued on an upward path, including further tours plus MSc and PhD degrees from The Ohio State University. He moved to the Defense Mapping Agency (DMA), as NGA was then, working on satellite imagery, and was assigned to the Mapping and Charting Establishment in the London suburbs. This led to the second trauma. Work went well, but the children had to attend public school in a deprived area of London, while the British officers' offspring enjoyed private schools. The experience was desperate, with bullying rife and sympathy all but absent. The Maune family beat an urgent retreat to the US – and indeed one of his successors did the same. The whole episode makes for harrowing reading, but worse was to come. The distress from the children's ordeals triggered his wife's mental illness, paranoid schizophrenia manifested by the hearing of voices, because of which Maune became her selfless carer for 46 years.

These occurrences, early in Maune's career and revealed in the first third of the book, linger in the reader's mind, but underline Maune's courage, resourcefulness and resilience, helped by his religious convictions, themselves crystallized by the attack in Vietnam. There is no space here to document Maune's achievements during his Army years: *LIDAR Magazine* folk will want to read these for themselves.

Maune left the Army and, after unsuccessful attempts to secure employment at DMA or The Ohio State University, joined Dewberry in 1992, where he toiled for long hours for 26 years. Like Maune's accounts of his Army years, those of his Dewberry years include fascinating insights into the history of surveying and mapping. Your reviewer was pleased to read about its use of BAE Systems' SOCET SET software. Once again, readers will want to peruse this for themselves. Maune's Dewberry years are perhaps best known for his authorship or co-authorship of many major government reports. The most familiar ones led to nationwide elevation data, most recently in the almost complete 3DEP program, but there were many others. These are not easy to write and often involved preparing, circulating and analyzing questionnaires about user requirements. Maune's account of the justification, preparation and influence of these documents is unexpectedly engaging. He comes over as someone who would go into the office, immerse himself at his desk and on the telephone for 12 hours and be endlessly productive. No doubt he was!

During the Dewberry years, his elder daughter Cherie died of cancer in 2005 at age 41. Again, Maune drew on his resources and fought on. Throughout the book he is generous in his praise of colleagues – supervisors, equals and subordinates alike. He and his family have given generously of both time and funds in volunteer and charity work. Then, well into the autumn of his years, he met Jewel McKee, a friend through church, and commenced a second marriage in April 2022 at the age of 83. His accounts of their relationship and times together are heartwarming. He retired from Dewberry at the end of that year, though he remains on call. One feels that he deserves happiness after a life of hills and valleys.

The book is enhanced by two useful appendices. The first summarizes technology changes during Maune's mapping career and consists of quick summaries of what has changed in ten different areas, for example cartography, photogrammetry and accuracy standards. For readers not well versed in geospatial history, this is a useful starting point, even if it is from the perspective of the author. The second appendix covers business uses and benefits of DEMs, no less than 30 of them, ending with a tabulation of annual dollar benefits. This sort of analysis is at the center of Maune's expertise.

The book ends with seven pages of acronyms and initialisms. These would have been less had Maune not been in military service for many years!

Maune has produced a successful autobiography. Your reviewer's copy was received directly from the author and is inscribed with Maune's adage, "May all your DEMs come true." It's not easy to combine the details of a personal life with accounts of complex technologies with which many readers may be unfamiliar. But as long as the reader has at least a passing interest in the world of surveying and mapping, then the formula works. Some of the many personal photos, especially those of Maune's relatives, may be of limited interest to most readers, but they do convey a flavor of the author's life. And those parts of the book where Maune described the difficulties that he and his family encountered are hard to read yet riveting. Most readers of *LIDAR Magazine* will be aware of Maune's more recent achievements and contributions; now they know the man behind them and can understand and admire the full and faithful life that he has enjoyed. He has had 86 remarkable years. May he have many more.

BY STEWART WALKER

# 25¢ Piano Lessons

David Maune is an American lidar hero well known to readers of *LIDAR Magazine*, which had the honor in 2018 of presenting him with the Lidar Leader Award for Outstanding Personal Achievement. The author holds this in high regard and devotes chapter 22 of this autobiography to the topic.

This is not a lidar book. It's a personal account of a life well lived, of family, of sadness, of remarkable achievements. Yet amongst Maune's numerous accomplishments, surely his studies of the return on investment of national elevation data in the US must rank high. As he shows in chapter 18, the 3DEP program is almost complete and the US is blessed with an enviable, authoritative elevation dataset that is available free-of-charge to the multiplicity of users who are thereby enabled to develop science, protect and empower the citizenry, and refine the remarkable technology that made it all possible – lidar.

The book is easy reading, with short chapters, and is lavishly illustrated, mainly from the author's personal photo albums. It is divided into four parts: "My Early Years" (5 chapters), "My Army Years" (9), "My Dewberry Years" (9) and "Count My Blessings" (7).

Maune was born in 1939 in Washington, Missouri, a river-crossing town. His father's grandparents had emigrated from Germany in the 1840s. Maune grew up in a family of very modest means, but not in hunger or grinding poverty. Nevertheless, his parents had to scrape to afford the piano lessons they gave him in 1947, which are memorialized in the title of the book. He practiced on a piano that was a gift from another family. Maune returns to these lessons in the final chapter of the book and expresses his gratitude that they not only engendered his love of music, but helped him meet his wife and find his way into a military career.

After high school, Maune embarked on the path that would shape his life. For those of us mollycoddled by European socialist paraphernalia such as low-cost or free higher education, this is an inspiring, curiously American episode. Eschewing the offer of a Catholic seminary, Maune opted for the Missouri School of Mines, following his brother there. He carried out minutely detailed budgeting in advance, as part of which he committed to the Reserve Officers' Training Corps and the career of an Army officer, in order to enhance the income side.

Maune married Mary Ellen Hill in 1961. His honesty is astonishing and leads to tough reading as he described an "unromantic" honeymoon owing to religious convictions. This led to a pragmatic change of denomination. Meanwhile Maune graduated, became an Army officer and carried out duties around the world for 30 years. His daughters were born in Fort Leonard Wood, Missouri and Heidelberg. Travel and living conditions were of variable quality – indeed, the Army's HR side hardly emerges from

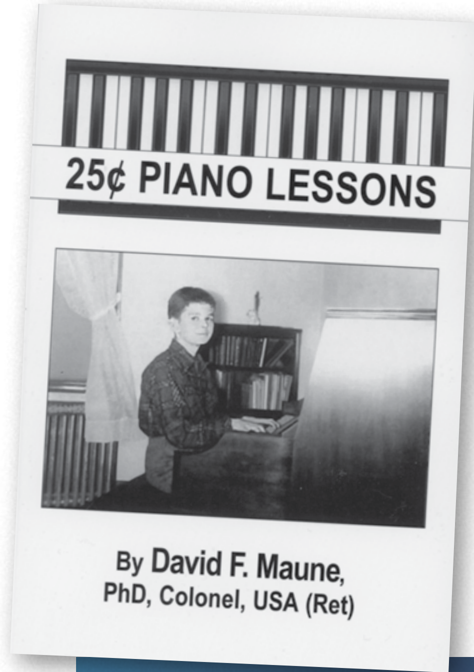


**25¢ PIANO LESSONS**

DAVID F. MAUNE

- Published by David F. Maune, PhD, Colonel (Ret.), Alexandria, Virginia, 2024
- 229 x 153 mm, x + 294 pp, numerous color and black and white illustrations
- Paperback, ISBN 979-8-218-54226-9, $24.95 from Amazon in US

this book with flying colors – yet Maune's realism and energy triumphed and life was interesting and productive. Military duties gave rise to two life-changing episodes in Maune's colorful life. In 1966, while serving with the 569th Engineer Company (Topographic) near Saigon, he was wounded in a Viet Cong grenade attack and attributes his survival (after extensive medical treatment) to God as his guardian angel. This gave his life purpose – something to which he returns frequently throughout the book.

*continued on page 46*

# SNOOPY LiDAR

The Multi-Platform LiDAR System Trusted Since 1999
Options Include Fully NDAA for Surveyors, Engineers,
Government and Education Applications.

MMS ENABLED

NDAA COMPLIANT

SINCE 1999

LiDAR USA

SURVEY GRADE LIDAR SYSTEMS DESIGNED BY REAL SURVEYORS